JNC TN8430 99-009

COUPLED THERMO - HYDRO - MECHANICAL EXPERIMENT AT KAMAISHI MINE

TECHNICAL NOTE 14-99-01

VERIFICATION OF THE BUFFER MATERIAL EMPLACEMENT TECHNIQUE

Y. Sugita, M. Chijimatsu and T. Fujita
Japan Nuclear Cycle Development Institute (JNC)

P.O. Tran Duc
HAZAMA Corporation

JNC TN8430 99-009
１ ９ ９ ９ 年 ６ 月

釜石原位置試験場における粘土充填・熱負荷試験
テクニカルノート　14-99-01
粘土施工技術の検証

（試験報告）

杉田裕*1，千々松正和*1，藤田朝雄*1，トランドュク・フィ・オアン*2

要　旨

地層処分における技術開発の観点からは、工学規模での試験によるニアフィールド環境である周辺岩盤の挙動が人工バリアに与える影響の把握および周辺岩盤を含むニアフィールド性能の定量的評価と室内および原位置における大型試験による人工バリアの品質性能の確認を行い、地層処分技術の信頼性向上を図ることが重要となっている。そのため、核燃料サイクル開発機構東海事業所の地層処分基盤研究施設等における工学規模の試験と並行して、原位置試験場において、人工バリアの品質性能の確認およびその実岩盤条件下でのニアフィールド連成挙動を評価することが必要となっている。

そこで、実条件でのニアフィールド環境を把握するため釜石原位置試験場において粘土充填・熱負荷試験を実施してきた。

粘土充填・熱負荷試験において緩衝材の充填方法の一つである現場締固め方式のまきだし・転圧工法を実施し，施工性および品質を実岩盤条件下で確認した。試験は実規模室内試験および原位置試験で構成し，実規模室内試験では材料を均一かつ高密度に充填するための技術開発を行った。

実規模室内試験において設定した諸条件に基づいて試料を充填した原位置試験では，粘土充填・熱負荷試験で充填目標値とした乾燥密度（管理値は 1.60-1.70g/cm^3 ）でベントナイト単体試料を施工することが可能であった。

*1　東海事業所　環境保全・研究開発センター　処分研究部　処分バリア性能研究グループ
*2　株式会社　間組

JNC TN8430 99-009
June, 1999

COUPLED THERMO-HYDRO-MECHANICAL EXPERIMENT AT KAMAISHI MINE
TECHNICAL NOTE 14-99-01
VERIFICATION OF THE BUFFER MATERIAL EMPLACEMENT TECHNIQUE

ABSTRACT

It is an important part of the near field performance assessment of nuclear waste disposal to evaluate coupled thermo-hydro-mechanical (T-H-M) phenomena, e.g., thermal effects on groundwater flow through rock matrix and water seepage into the buffer material, the generation of swelling pressure of the buffer material, and thermal stresses potentially affecting porosity and fracture apertures of the rock. An in-situ T-H-M experiment named "Engineered Barrier Experiment" was conducted at the Kamaishi Mine, in which the host rock is granodiorite, in order to establish conceptual models of the coupled T-H-M processes and to build confidence in mathematical models and computer codes.

This report summarizes the results of the in-situ direct compaction technique to evaluate the appropriate conditions for this technique. The in-situ direct compaction technique is one of the major candidate emplacement techniques for the buffer material. This experiment consisted of the mock-up tests and the in-situ test. The mock-up tests showed the appropriate conditions for the in-situ direct compaction technique. For the in-situ experiment, the manufactured OT-9607 achieved dry density averaged 1.65 g/cm^3, which matched the demand for the thermo-hydro-mechanical experiment.

COUPLED THERMO-HYDRO-MECHANICAL EXPERIMENT AT KAMAISHI MINE
TECHNICAL NOTE 14-99-01
VERIFICATION OF THE BUFFER MATERIAL EMPLACEMENT TECHNIQUE

CONTENTS

1. INTRODUCTION

A buffer material was emplaced around the High-Level Radioactive Waste package(HLW) in the engineered barrier. The Buffer material has the some performances; low hydraulic conductivity, swelling characteristics, stress buffer and so on. These performances depend on dry density of the buffer material. There is a need to develop the adequate emplacement technique of the buffer material. The typical emplacement techniques of the buffer material are block-type emplacement technique and in-situ direct compaction technique (divided into spreading and rolling compaction technique and spraying technique).

Block-type emplacement technique was conducted in a buffer mass experiment of STRIPA PROJECT in Sweden (Pusch and Börgesson, 1985), BACCHUS backfill experiment at Mol in Belgium (Neerdael et al., 1992), Buffer/container experiment at URL in Canada (Kjartanson et al., 1993), Big-Ben in man-made rock (reinforced concrete) in Japan (Sato et al., 1991) and so on. With regard to the in-situ direct compaction technique, spreading and rolling compaction technique was conducted in field test of tunnel backfilling at ÄSPÖ in Sweden (Gunnarsson et al., 1996). In spraying technique, fundamental experiment of bentonite-sand mixture was conducted in Japan (Sugita et al., 1995).

Regarding superior points of each technique, in block type, high density and high swelling block will be manufactured by a high performance machine. In the direct compaction technique, there will be no gap between rock and the buffer material, and the buffer material and HLW.

For the verification of the emplacement technique of the buffer material, the quality of the block emplacement technique depends upon the compaction machine and handling methods. However, in the Kamaishi experiment, the size of the drift and the capacity of the transportation restricted the machines. On the other hand, environmental conditions will influence the quality and the emplacement in the direct compaction technique. Therefore, it was needed to conduct the direct compaction technique to clarify the subjects.

In this case, direct compaction technique was selected to emplace the buffer material into the test pit of the coupled T-H-M experiment at Kamaishi experiment.

2. CONTENTS OF EMPLACEMENT EXPERIMENT

2.1 EMPLACEMENT OF THE BUFFER MATERIAL

Uniform emplacement of the buffer material was required to perform a coupled thermo-hydro-mechanical experiment, because distribution of dry density and water content of the buffer material would influence the monitoring data about the coupled T-H-M phenomena. In this case, the direct compaction technique was selected to emplace the buffer material. And, the restrictions of transportation of the machines and the conditions of the drift did not permit the use of a heavy-duty compaction machine. Therefore, the buffer material was spread into the test pit, and set up by rolling compaction with the electric rammer.

Mock-up tests were performed to investigate the optimum conditions to emplace the buffer material into the test pit. This test was performed at Big-Ben in the Japan Nuclear Cycle Development Institute (JNC) Tokai works. Big-Ben has a reinforced concrete body and a full sized test pit, 1.74m in diameter and 5.0m in depth. In this pit, the same conditions of emplacement as in-situ reappeared.

Figure 2-1 shows the procedure of emplacement experiment of the buffer material. This experiment consisted of mock-up tests and in-situ test. Mock-up tests had compaction depth tests that determined the spreading depth of each layer, dry density tests that noted the distribution of dry density on a layer, and water content tests that investigated the optimum water content of the buffer material. Adequate conditions that were derived from the results of mock-up tests were applied to the in-situ test.

2.2 SPECIMEN

The specimens were bentonite Kunigel V1 (hereinafter called "Kunigel V1"), bentonite-sand mixture and bentonite OT-9607 (hereinafter called "OT-9607", Fujita et al., 1997). Sand of bentonite-sand mixture was a blend of silica sand #3 and pearl sand #5. The well-graded specimen was needed to obtain the good compactibility and high dry density of the buffer material. The mixture of sands of various grain sizes is effective to obtain a well-graded specimen. Figure 2-2 shows the grain size accumulation curves of various sands as silica sand #3, pearl sand #5, silica sand #7 and mixtures. The #3+#5+#7 was the best well-graded mixture. However, the mixture of two kinds of sands is better than the mixture of three kinds of sands to provide a number of uniform specimens with grain size distribution. The grain size of Kunigel V1 is smaller than that of the sands. Therefore, the blend of silica sand #3 and pearl sand #5 was selected for this test.

Table 2-1 shows the characteristics of sample as bentonite, sands and mixture. The mixture of silica sand #3 and pearl sand #5 was in the ratio of 1:1 by weight. The mixture of Kunigel V1 and the mixture sand was in the ratio of 7:3 by weight.

Usually, the bentonite under 250 mesh is collected as "the bentonite Kunigel V1" in the bentonite plant in Tukinuno. However, OT-9607 is the special named for this test. The crushed bentonite was classified according to a particle size. The size under 2 mm was collected as OT-9607 in the plant. OT-9607 had the same chemical composition as Kunigel V1. Figure 2-3 shows grain size accumulation curve of OT-9607 which is the well-graded specimen; the same as mixture #3+#5+#7.

Figure 2-4 and 2-5 show the compactibility of the specimen in the laboratory test. Figure 2-4 shows the compactibility of bentonite. In compaction energy as 15 Ec (1 Ec=5.49E5 J/m^3), the maximum dry density of Kunigel V1 is about 1.75 g/cm^3 when the optimum water content is 13.5 %; that of OT-9607 is about 1.95 g/cm^3 when the optimum water content is 11.0 %. For Kunigel V1, when a much larger compaction energy is applied, the optimum water content becomes lower. This tendency was applied to OT-9607 also. Figure 2-6 shows the compactibility of bentonite-sand mixture. Compaction energy is 1 Ec. Specimen of mixture #3+#5+#7 obtained the greatest maximum dry density, but accomplished dry density of all specimens are almost the same. The selected specimen for the emplacement, mixture #3+#5, displayed a dry density of 1.6 g/cm^3 at an optimum water content of 18.2 %.

Hereinafter, Bentonite-sand mixture means the mixture Kunigel V1 and mix of silica sand #3 with pearl sand #5. Bentonite-sand mixture was applied to compaction depth tests and dry density tests. Kunigel V1 and OT-9607 were applied to water content tests. And, OT-9607 was applied to the in-situ test. The energy of a compaction machine for mock-up tests and in-situ test was greater than the one used for the laboratory test. From the results of the compactibility test in laboratory, the greater the compaction energy applied, the smaller the optimum water content becomes. Therefore, the water content of specimen was arranged adequately for mock-up tests and in-situ test.

Table 2-1 Characteristics of sample

Sample	Specific gravity	Water content (%)	Chemical composition (%)	Texture			
				Dmax (mm)	D_{10} (mm)	Fine-grained ratio Fc (%)	Uniformity coefficient Uc
Kunigel V1	2.6	<10	SiO_2 : 70.2 Al_2O_3 : 14.2 Fe_2O_3 : 2.5 CaO : 2.0 MgO : 2.2 Na_2O : 2.5 K_2O : 0.2 I.L : 4.6	250 mesh; through abobe 90%			
OT-9607	2.6			4.75	0.19	0.8	3.8
Silica sand #3	2.65	0.12-0.14	SiO_2 : 99.8 Al_2O_3 : 0.05 Fe_2O_3 : 0.01 MgO : 0.01 Na_2O : 0.01 K_2O : 0.01 TiO_2 : 0.03 I.L : 0.12	4.75	0.93	0	1.4
Pearl #5	2.66	0.12-0.14		2.0	0.31	0	1.6
#3+#5	2.64	0.12-0.14		4.75	0.35	0	2.8

$Uc=D_{60}/D_{10}$; Gradient of grain size accumulation curve. Near 1 is poorly-graded.
Dmax ; maximum grain size
D_{10} ; 10 percent diameter
D_{60} ; 60 percent diameter
Fc ; 0.075mm passing

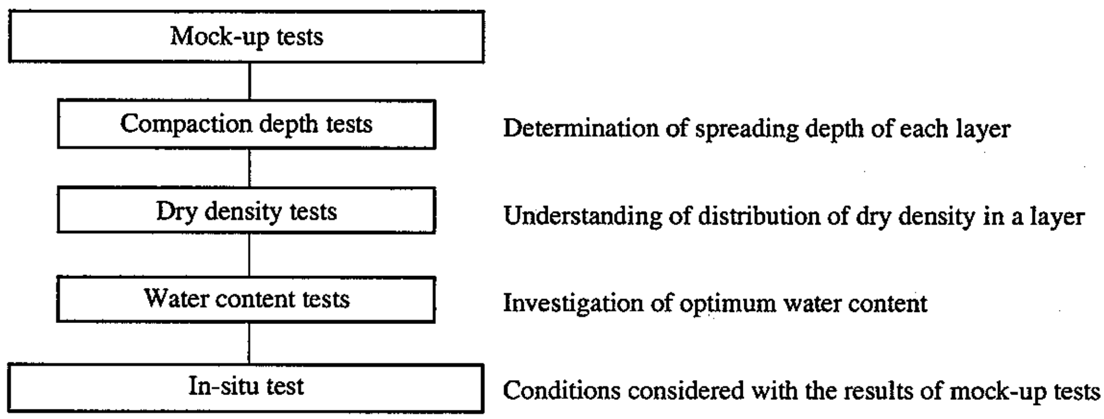

Figure 2-1 Procedure of emplacement experiment of buffer

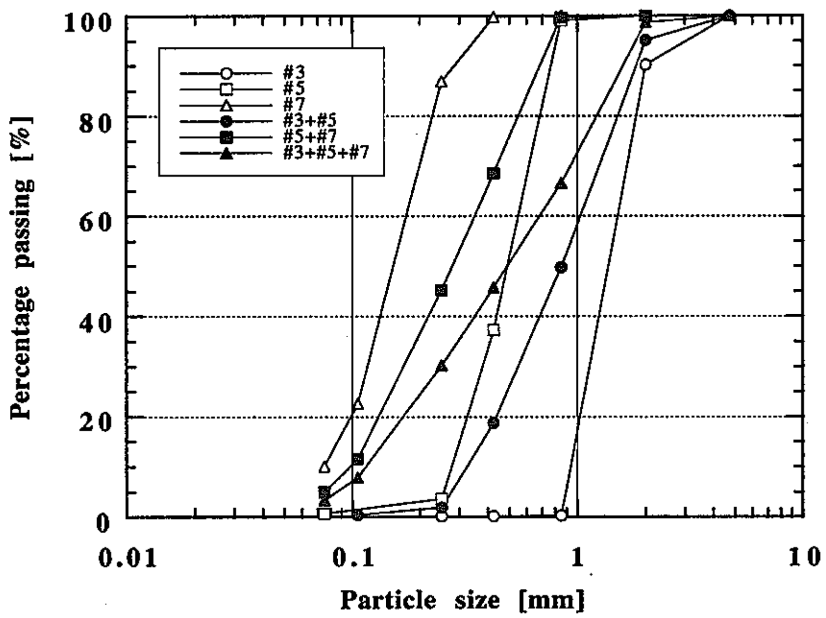

Figure 2-2 Grain size accumulation curve of quartz sand

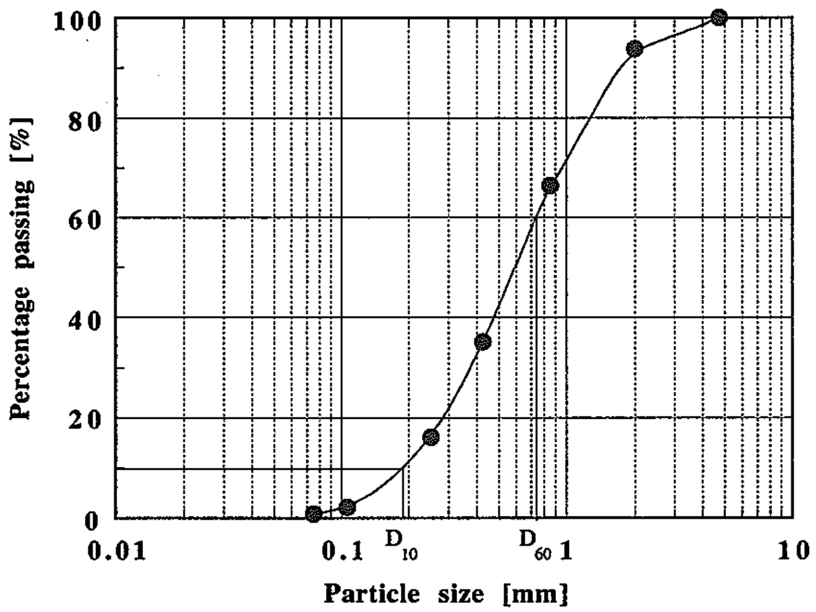

Figure 2-3 Grain size accumulation curve of OT-9607

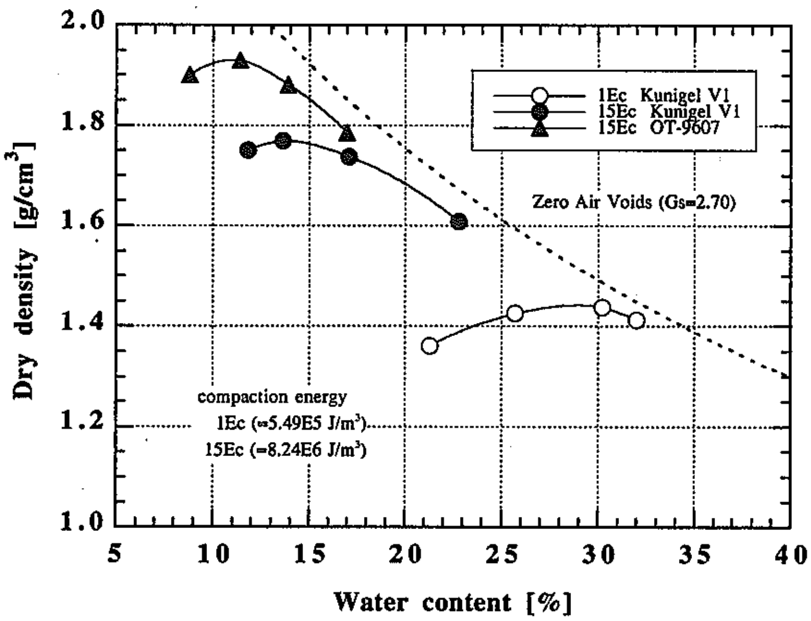

Figure 2-4 Compaction curves of Bentonites

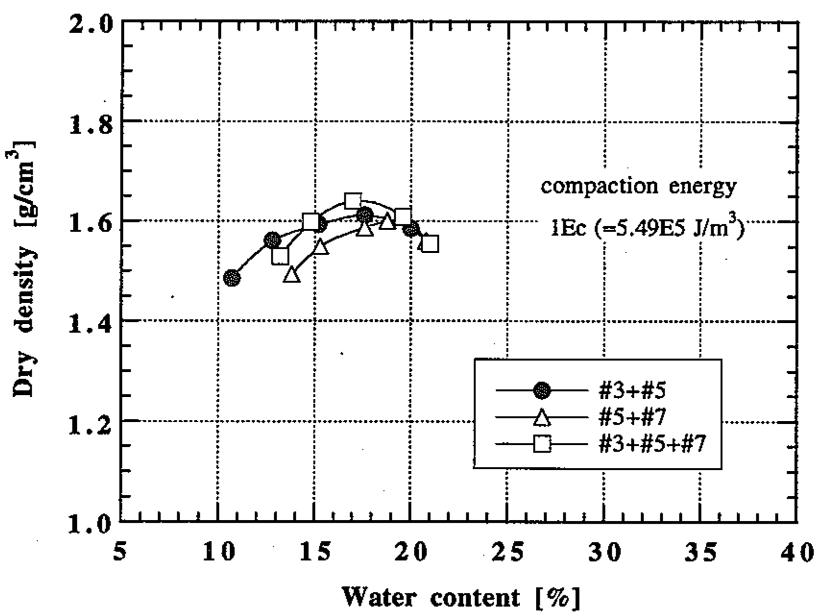

Figure 2-5 Compaction curves of bentonite-sand mixtures
(Kunigel V1 : Sands ratio = 70:30)

3. MOCK-UP TESTS

3.1 COMPACTION DEPTH TESTS

Compaction depth tests were performed to determine the adequate spreading depth for each layer. In the case of the thin layer, compaction energy is effectively applied to the whole layer, and the density of the layer becomes higher. However, the cycles of spreading of specimen and treatments between layers increase. In the case of the thick layer, it is considered that rolling compaction doesn't converge and that the controlled dry density is not achieved. It is needed to determine the adequate spreading depth of a layer.

Bentonite-sand mixture was a blend of Kunigel V1 and sands. This specimen was mixed for 5 minutes using a vertical shaft type mixer at 90 r.p.m. One batch was about 40 kg and the initial water content was about 15 %.

The selected tests incorporated the three depths of spreading of specimen; 5, 10 and 15 cm. Convergent rolling compaction time of each depth was measured, and the adequate depth was determined. After rolling compaction, sampling tests were performed. The samplings observed the distribution of dry density and water content, and the uniformity in a layer. Figure 3-1 shows the procedure of compaction depth tests. At first, the base layer was compacted. The base had two layers and the thickness of each layer was 10 cm. The base layer simulated the end of compaction of a certain layer, because the bottom of test pit of Big-Ben was reinforced concrete.

First, the layer thickness was 5 cm. Specimens were spread uniformly on a layer, and rolling compaction applied using electric rammer. Figure 3-2 shows the electric rammer (Mikasa, MT-M50V) which weighs 48 kg. Compaction energy is from 750 to 850 kg/cycle. Impacting value is from 650 to 750 per minute. If the energy loss is 30 %, rolling compaction energy is 2.19E7 J/m^3. After compaction of two layers, a core cutter test (JGS 1613-1995, 1995) was performed on the points of Figure 3-3. The size of the core cutter was 7.5 cm in diameter and 6.5 cm in height. The samples of the core cutter were measured for dry density and water content.

Continuously, the layer of 10 cm in depth was compacted. Compaction procedure was the same as 5 cm. In this depth, only one layer was compacted. Core cutter test was performed on the points of Figure 3-3 after compaction of the layer. The samples of core cutter were measured for dry density and water content.

Last, the layer of 15 cm in depth was compacted. Compaction procedure was the same as 5 cm. For this depth, one layer was compacted. The core cutter test was performed on the points of Figure 3-3 after compaction of the layer. In this case, the samples of the points of -4 cm (triangle mark) and -8 cm (square mark) from the surface were measured to observe the distribution of dry density in the cross-section.

3.2 RESULTS OF COMPACTION DEPTH TESTS

Figure 3-4 shows the relationship between settlement of the specimen and rolling compaction time on each depth, 5 cm, 10 cm and 15 cm. In all cases the specimen was compacted quickly, then settlement of specimen converged. The convergent times were about 25 minutes in 5 cm depth, about 50 minutes in 10 cm, and about 100 minutes in 15 cm. Figure 3-5 shows the relationship between the depth of the layers and convergent time of rolling compaction, and compaction cycles for 100 cm in depth. The convergent time increased with the depth of layer. The depth of specimen was inversely proportional to compaction cycles.

Figure 3-6 shows the relationship between depth of layer and dry density. On the surface, the accomplished dry density increased with the depth of layer. Before these tests, it was expected that a depth of 5 cm accomplished the highest dry density. It was considered that a thin layer was superior to conduct the applied compaction energy to the whole layer. The accomplished dry density showed the opposite tendency. On distribution in the cross-section of dry density, the points of surface and -3 cm were almost the same value for the 10 cm depth. For the 15 cm depth, the dry density of a deep point was smaller than that at the surface. The gradient of dry density appeared in the layer. It was considered that the compaction energy didn't conduct completely lower part. The depth of 15 cm, that had distribution of dry density in the layer, was eliminated from the following considerations.

Figure 3-7 shows the relationship between water content and dry density in the layer and the results on the surface. For the depth of 5 cm, the water content was 16 % or less. The dry density was 1.7 to 1.8 g/cm^3 and varied widely. In the depth of 10 cm, water content varied widely, but the dry density was almost 1.8 g/cm^3. It was noted that a spreading of the specimen affected the dry density. If an error range is the same, the error ratio to the depth of a layer depends on the depth of the layer. Therefore, the deeper layer is advantageous to set up the uniform layers.

From the results of spreading depth tests, the adequate spreading depth of a layer was 10 cm, and rolling compaction time was about 50 minutes.

3.3 DRY DENSITY TESTS

Dry density tests were performed to confirm the quality of the compaction layer using some measurement methods. Figure 3-8 shows the procedure of these tests. The first layer of 10 cm depth was compacted using the electric rammer for 50 minutes. Then, second and third layers were compacted. Total depth of the layer was 30 cm. Then, the level of the surface of the top plane was measured on the points of Figure 3-9. A core cutter test was performed on the points of Figure 3-9. The sampling points of the core cutter were 8 in number. Six points were on surface of the layer and 2 points were 3 cm from the surface. After measurement of the dry density using core cutter and level surveying, continuously, three layers were compacted. Total depth of layer became 60 cm. Dry density was measured using the core cutter and RI method (JGS 1614-1995) by the sand replacement method (JIS A 1214-1995) and level surveying. Water content was the measured. In addition, the grain size distribution was measured to observe the distribution of the sand ratio in the layer.

3.4 RESULTS OF DRY DENSITY TESTS

Figure 3-12 shows the distribution of dry density on the surface plane and in the cross-section of the layer which was 30 cm in depth. Dry density on the surface was 1.8 to 1.9 g/cm^3. The dry density of the center part of the test pit was higher than the outer part. It was considered that the compaction of the center using the electric rammer was complete, however the compaction of the outer part, especially closer to the rock mass, was incomplete. Regarding the distribution of dry density in the cross-section of the layer, dry density decreased with depth. This tendency was the same for the results of compaction depth tests. Point No.1 near the center of the test pit was uniform, and had high dry density. Dry density of point No.3 closer to the concrete wall varied widely with depth. However, there was no point with a dry density of 1.5 g/cm^3 or less.

Figure 3-13 shows the dry density using core cutter and RI method, by the sand replacement method and level surveying on the layer to 60 cm in depth. In the level surveying, dry density was 1.78 g/cm^3. The highest point of dry density in the surface was the middle point between the center and the outer part of the test pit. The measured value using core cutter was the highest in the all measurement methods. The measured value using a RI method and by level surveying was almost the same. The measured value by the sand replacement method was the lowest. It was considered that the density in core cutter increased when the core cutter was hammered into the layer. Roughness of surface of measurement points affected the accuracy of the sand replacement method. The measured value using RI method was used to measure mean dry density.

Figure 3-14 shows the distribution of the sand ratio in the layer. In the rolling compaction using impact type compactor as rammer, it was considered that the vibration caused the scatter of the sand ratio in the layer. The measured values in the plane were 29 to 31 wt%. In the cross-section, there were few measurement points nearby, however the values were almost the same. Therefore, the distribution of sand in the layer was uniform, and the layer was considered to be uniform.

3.5 WATER CONTENT TESTS

On compactibility of the buffer material, water content is one of the most important factors. Water content tests were performed to investigate the influence of the change of water content on the compactibility. The specimens were pure bentonite, Kunigel V1, and OT-9607. Figure 3-15 shows the results of the tests. These tests consisted of a bucket test and regular tests. A bucket test was conducted to determine the conditions for regular tests.

3.5.1 BUCKET TEST

The bucket was made of pipes and plywood. Water contents of the specimen were 10, 12 and 15%. A spreading specimen was compacted using the electric rammer, and the depth of each layer was 10 cm.

3.5.2 REGULAR TESTS

Water contents for these tests were determined with the results of the bucket test. Specimens were two kinds of Kunigel V1 (water content; 14, 16%) and three kinds of OT-9607 (water content; 12, 14 and 16%). Two layers of each specimen were compacted using the electric rammer. Dry density was measured a using RI method that was scatter type, and by work progress.

3.6 RESULTS OF WATER CONTENT TESTS

3.6.1 RESULTS OF BUCKET TEST

Figure 3-17 shows the situation of compaction of the bucket test. Two men operated the rammer to compact the spreading specimen. Table 3-1 shows the results of this test. With a water content of 10 %, much dust was present. Specimen remained powders, and compaction was incomplete, therefore, dry density was not measured. For the case of a water content of 12 %, compactibility was good. However, the surface of the layer had some cracks. This case wasn't adequate for emplacement of the buffer material. For the case of water content of 14 %, compactibility was very good. There was little dust and the surface of the layer was smooth. The data of dry density were measured with all measurement methods.

3.6.2 RESULTS OF REGULAR TESTS

In regular tests, compaction depth of each layer was 10 cm. Every case had 2 layers. First layer was for observation of rolling compaction time, and second layer was compacted as the same time. Specimen of case 1 was Kunigel V1 (water content : 16%), case 2 was Kunigel V1 (water content : 14%), case 3 was OT-9607 (water content : 12 %), case 4 was OT-9607 (water content : 14 %) and case 5 was OT-9607 (water content : 16 %). Figure 3-18 shows the compactibility of all cases. Settlement of all cases converged in 60 minutes as almost the same as the time of the compaction depth tests. This same time for rolling compaction time indicates no influence of water content variations.

Table 3-2 shows dry density using RI method (the scattered type nuclear gauge). Accurate data were measured with complete contact between the sensor and the object. There was roughness on the surface of the compacted layer by rolling compaction. This roughness seemed to affect the scatter of the data. The measured values were considered to be lower than a calculated dry density. In regular tests, plural measurements (5 times in principle) were performed to observe the scatter of the data. The maximum error of the measured data between maximum and minimum was only 0.209 g/cm^3. Figures 3-19 to 3-23 show the distribution of dry density in the plane of each case. For a water content of 16 % in case 1 and case 5, the measured values were almost the same using RI method gauge and did not scatter. The layers in both cases were uniform. However, the accomplished dry density was only 1.3 g/cm^3 in case 1. In case 5, the accomplished dry density was about 1.65 g/cm^3. For water contents of 12 and 14%, the measured values using RI method were less than the values by work progress. Also, the dry density was less than the data in case 5. Table 3-3 shows the comparison of handling for each case. Regarding dust and cracks of surface, the obtained dry density in case 5 was the best of these tests. In case 1, the dry density using core cutter was measured. Figure 3-24 shows the comparison the data between using core cutter and RI method. The dry density using core cutter was larger than the value using RI method.

Figures 3-25 and 3-26 show the relationship between dry density and water content. Figure 3-25 shows the results of case 1 and case 2 for Kunigel V1. Figure 3-26 shows the results of case 3, case 4 and case 5 for OT-9607. In each case, water content did not scatter, and it was considered that the layer was controlled well. For dry density, the center parts were larger than the outer part. This was the same tendency as with the results of dry density tests. In each case, dry density increased with water content. Water contents of 15 to 16 % achieved the highest density. For Kunigel V1, there was the scatter of dry density between the center and the outer of the test pit. In each part, the data were almost the same. For OT-9607, the data were almost the same in every case. Especially, case 5 was considered to be the best condition.

The results of the mock-up tests determined the conditions for in-situ test.

1) Adequate spreading depth is 10 cm using the electric rammer.
2) 60 minutes is required for rolling compaction of a layer.
3) The level surveying measured the mean value of dry density of the layer.
4) The sand ratio in a layer of bentonite-sand mixture is uniform.
5) OT-9607 is useful specimen to accomplish the high dry density in pure bentonite.
6) Adequate initial water content is 15 %.

Table 3-1 Results of bucket test

sample			OT-9607			remark
target water content [%]			10	12	15	
measured water content [%]			9.3	11.9	13.9	
handling			Specimen remained powder. Compaction was incomplete. Many dusts happened.	Compactibility was well. Surface of layer had some cracks. Little dust happened.	Compactibility was very well. Handling was good. Surface of layer was smooth. Few dust happened.	
dry density	core cutter	wet density water content dry density saturation	impossible	not carry out	2.091 g/cm^3 13.9 % 1.836 g/cm^3 87-80 %	End of core cutter changed the shape.
	coaring	wet density water content dry density saturation	impossible	not carry out	2.021 g/cm^3 13.8 % 1.776 g/cm^3 77-72 %	replacement of core was very hard.
	RI method	wet density water content dry density saturation	impossible	not carry out	2.009 g/cm^3 14.1 % 1.761 g/cm^3 77-71 %	Pre drilling was needed.
	calculated average values	wet density water content dry density saturation	—	1.855 g/cm^3 11.9 % 1.658 g/cm^3 54-51 %	2.102 g/cm^3 13.8 % 1.874 g/cm^3 88-81 %	

Table 3-2 Measurement values of dry density using RI method (Water content tests)

Test case Measurement point	Scatter of data on the same point (using RI method) min. max.	diff.	mean	Scatter of mean value (g/cm³) min. max.	diff.	mean
Case1, center						
NO.1	1.275、1.308	0.033	1.284	1.268, 1.420	0.152	1.330
NO.2	1.262, 1.281	0.019	1.275			
NO.3	1.403, 1.417	0.014	1.404			
NO.4	1.258, 1.281	0.023	1.268			
NO.5	1.411, 1.425	0.014	1.420			
Case1, around						
NO.6	1.240, 1.258	0.018	1.250	1.030,1.250	0.220	1.174
NO.8	1.222, 1.237	0.015	1.230			
NO.10	1.183, 1.194	0.011	1.187			
NO.12	1.019, 1.036	0.017	1.030			
Case2, center						
NO.1	1.103, 1.131	0.028	1.116	1.108, 1.204	0.096	1.151
NO.2	0.955, 1.164	0.209	1.108			
NO.3	1.125, 1.209	0.084	1.204			
NO.4	1.170, 1.197	0.027	1.185			
NO.5	1.121, 1.157	0.036	1.140			
Case2, around						
NO.6	0.833, 0.848	0.015	0.842	0.800, 0.868	0.068	0.837
NO.8	0.839, 0.868	0.029	0.856			
NO.10	0.800, 0.816	0.016	0.812			
NO.12	0.829, 0.848	0.019	0.838			
Case3, center						
NO.1	1.382, 1.438	0.056	1.414	1.267, 1.456	0.189	1.359
NO.2	1.267, 1.273	0.006	1.269			
NO.3	1.387, 1.393	0.006	1.389			
NO.4	1.450, 1.460	0.010	1.456			
NO.5	1.220, 1.277	0.057	1.267			
Case3, around						
NO.6	1.411, 1.425	0.014	1.420	1.223,1.420	0.197	1.317
NO.8	1.211, 1.234	0.023	1.223			
NO.10	1.375, 1.407	0.032	1.390			
NO.12	1.387, 1.396	0.009	1.391			

Table 3-2 Measurement values of dry density using RI method (continued.)

(Water content tests)

Test case Measurement point	Scatter of data on the same point (using RI method)			Scatter of mean value (g/cm^3)		
	min. max.	diff.	mean	min. max.	diff.	mean
Case4, center						
No.1	1.503, 1.548	0.045	1.522	1.391, 1.522	0.131	1.454
No.2	1.383, 1.399	0.016	1.391			
No.3	1.452, 1.457	0.005	1.455			
No.4	1.392, 1.458	0.066	1.424			
No.5	1.374, 1.576	0.202	1.479			
Case4, around						
No.6	1.419, 1.421	0.002	1.420	1.246, 1.423	0.177	1.378
No.8	1.421, 1.426	0.005	1.424			
No.10	1.414, 1.426	0.012	1.421			
No.12	1.150, 1.335	0.185	1.245			
Case5, center						
No.1	1.660, 1.676	0.016	1.667	1.652, 1.668	0.016	1.662
No.2	1.654, 1.677	0.023	1.668			
No.3	1.658, 1.674	0.016	1.666			
No.4	1.645, 1.662	0.017	1.657			
No.5	1.644, 1.662	0.018	1.652			
Case5, around						
No.6	1.573, 1.614	0.041	1.592	1.551, 1.611	0.060	1.581
No.8	1.562, 1.588	0.026	1.571			
No.10	1.524, 1.575	0.051	1.551			
No.12	1.601, 1.622	0.021	1.611			

Table 3-3 Comparative valiation of handling on each case
(Water content tests)

Case	Specimen	Cracks	Dust	Compactibility	Handling
1	Kunigel V1 w=16.4%	△ (little)	△ (much)	△	△
2	Kunigel V1 w=14%	× (many)	× (much)	△	×
3	OT-9607 w=12.2%	△~× (many)	△ (much)	△	×~△
4	OT-9607 w=13.8%	△ (little)	○~△ (little)	△~○	△
5	OT-9607 w=15.8%	○ (few)	○ (few)	○	○

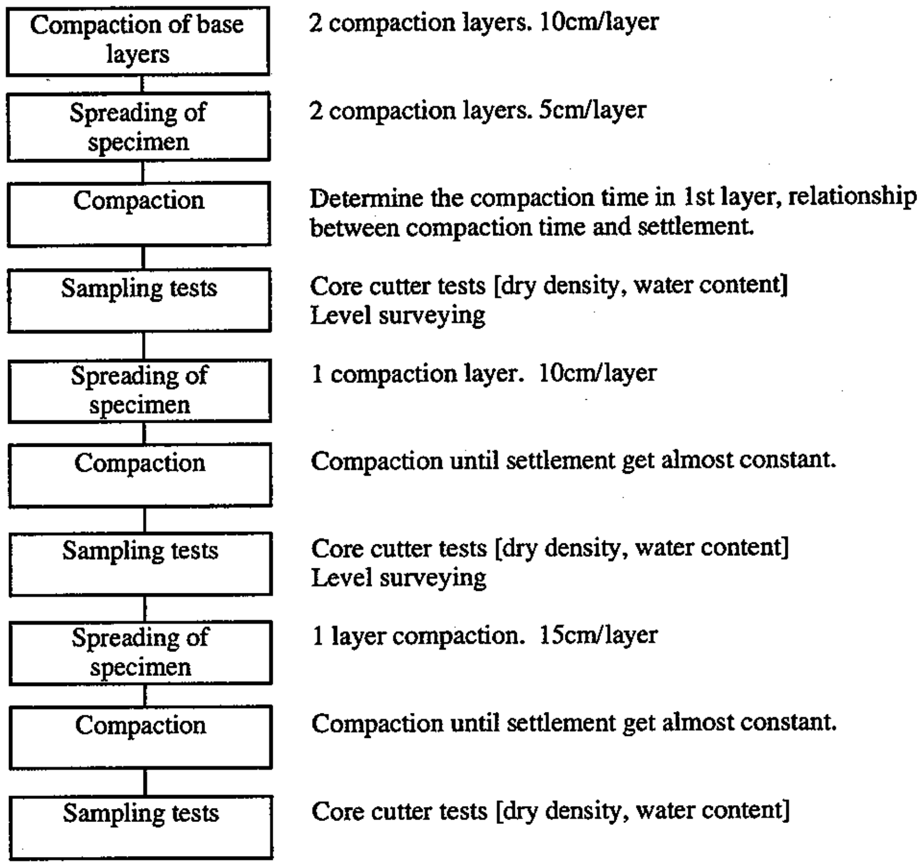

Figure 3-1 Procedure of compaction depth tests

Figure 3-2 Electric rammer

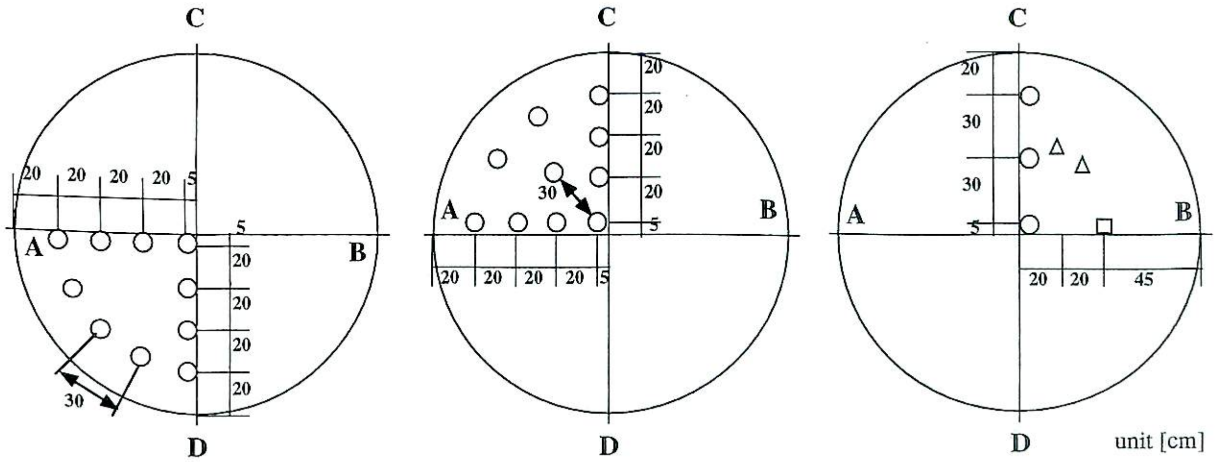

compaction depth : 5cm
(core cutter test)

compaction depth : 10cm
(core cutter test)

compaction depth : 15cm
(core cutter test)
△ -4cm
□ -8cm

Figure 3-3 Sampling points of dry density on a layer
(Compaction depth test)

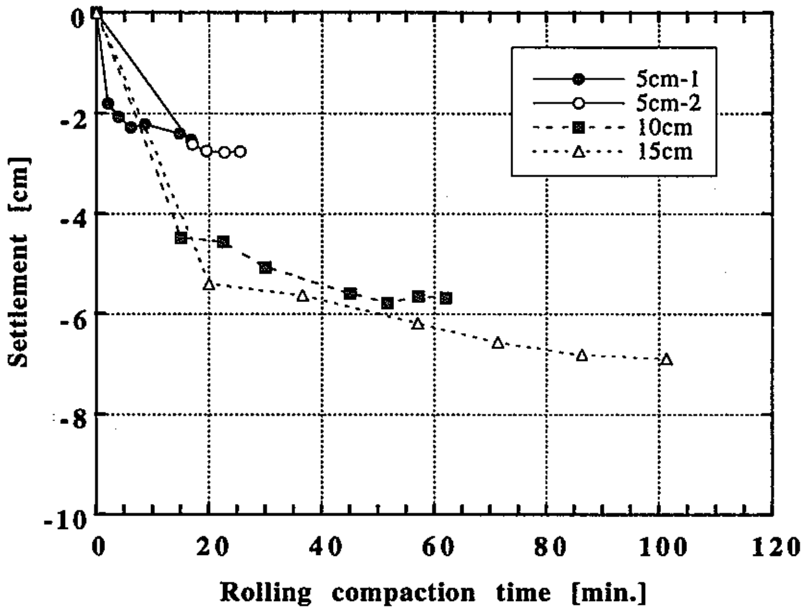

Figure 3-4 Settlement vs compaction time of bentonite-sand mixture

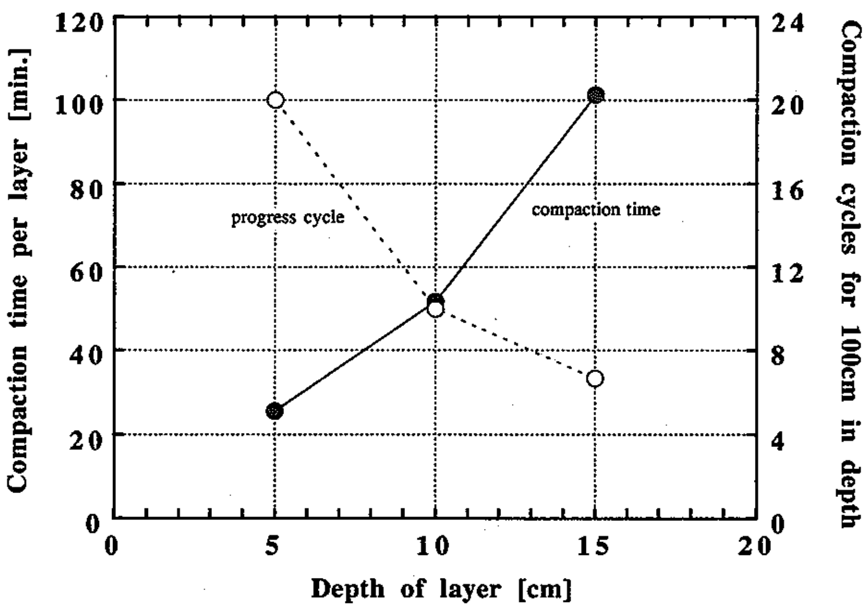

Figure 3-5 Compaction time per layer and Compaction cycles for 100 cm in depth vs depth of layer of bentonite-sand mixture

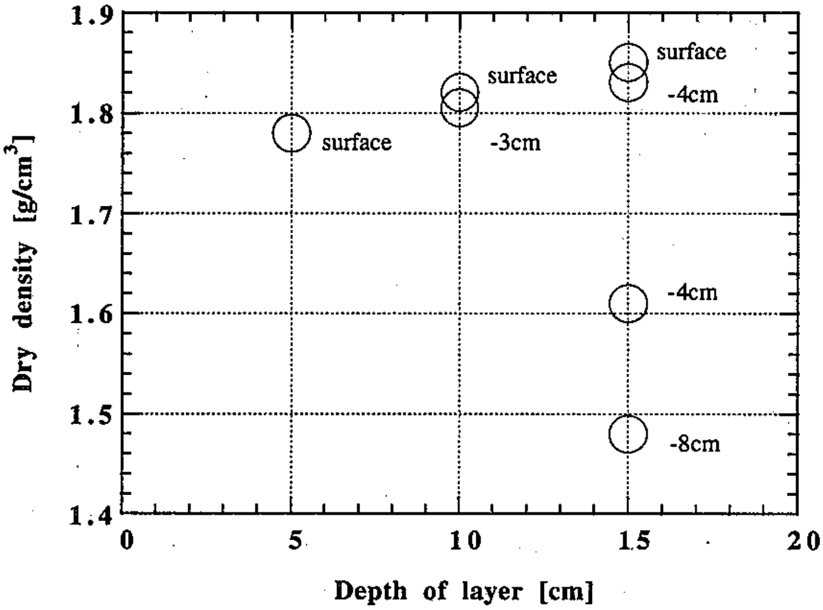

Figure 3-6 Dry density vs depth of layer
(core cutter test)

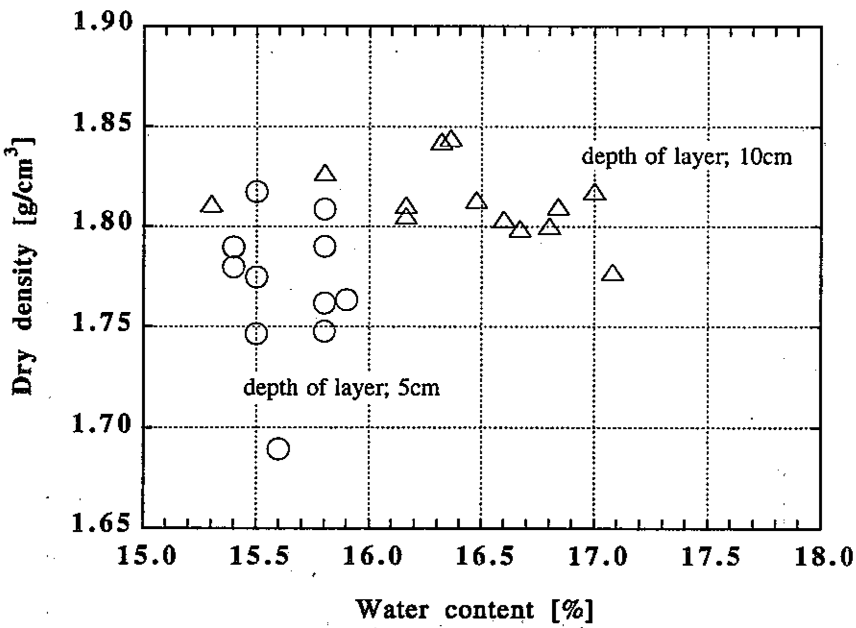

Figure 3-7 Dry density vs water content
(core cutter test)

Spreading of specimen	3 layers. 10cm/layer
Compaction	Electric rammer (48kg) Compaction time control
Work progress	Dept after compaction: 30cm
Sampling tests	Core cutter tests (dry density, water content) Level surveying
Spreading of specimen	3 layers. 10cm/layer
Compaction	Electric rammer (48kg) Compaction time control
Work progress	Dept after compaction: 60cm
Sampling tests	Core cutter tests (dry density, water content), level surveying, sand replacement method, RI method, laboratory tests

Figure 3-8 Procedure of dry density tests

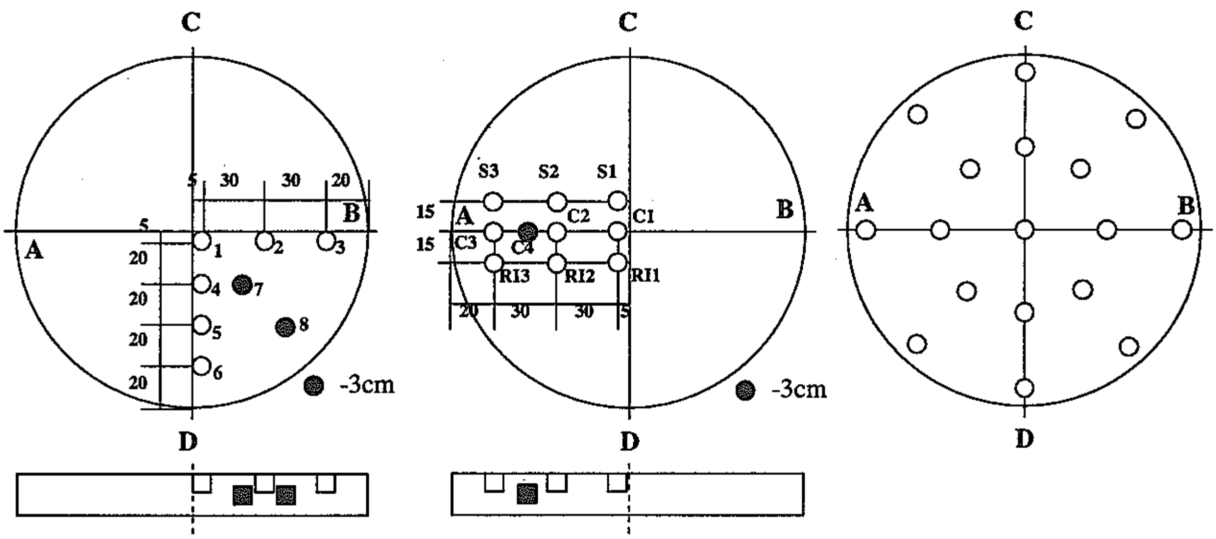

3rd layer
(core cutter test)

6th layer
C : core cutter test
RI: RI method
S : sand repllasement method

measurement points
of level surveying

Figure 3-9 Sampling points on a layer
(dry density tests)

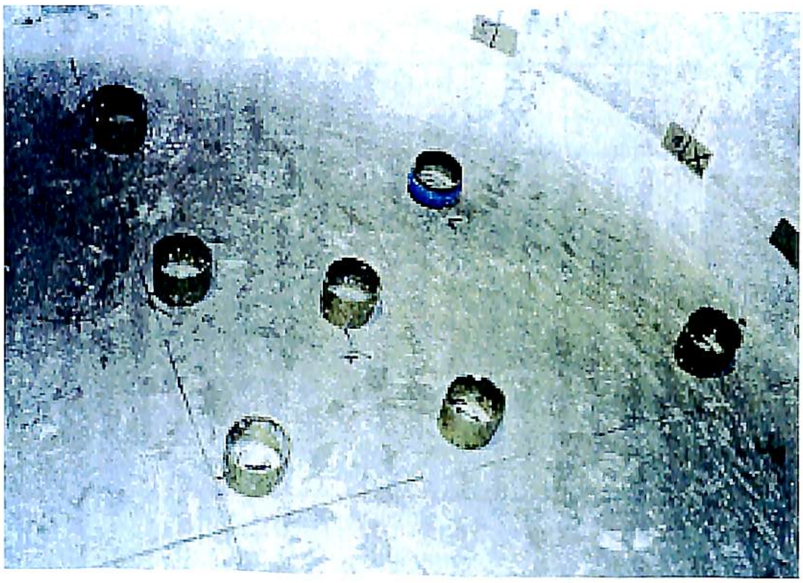

Figure 3-10 Schematic view of core cutter test

Figure 3-11 Schematic view of sand replacement method

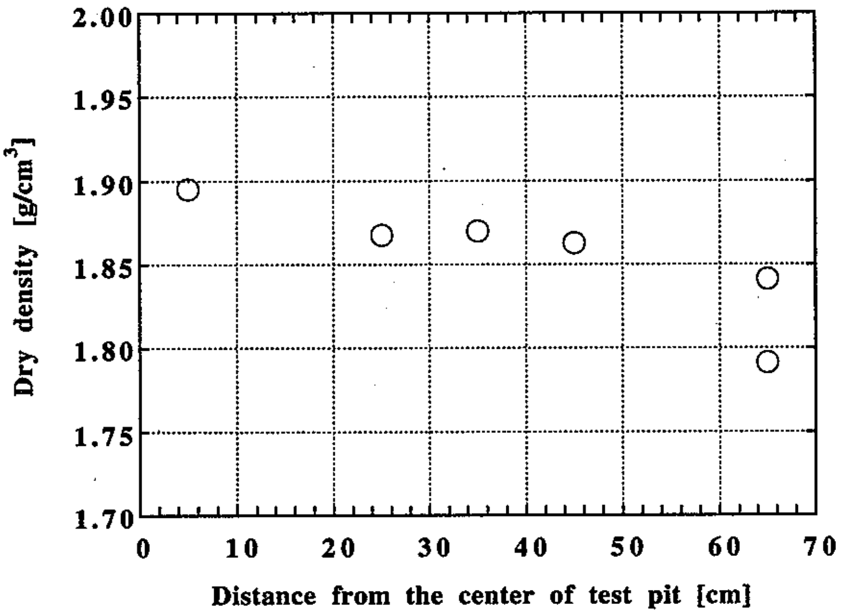

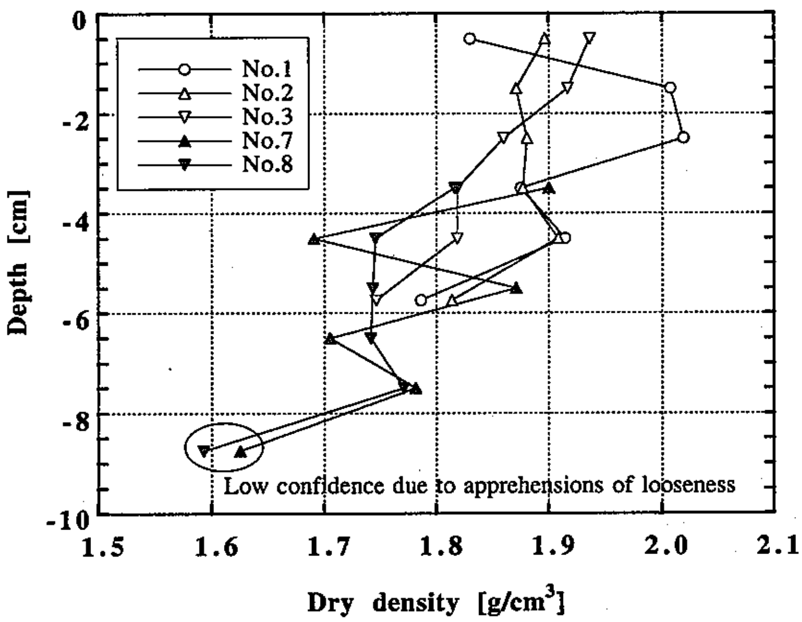

Figure 3-12 Distribution of dry density in depth of layer as 30cm
(upper; plane, lower; cross section)

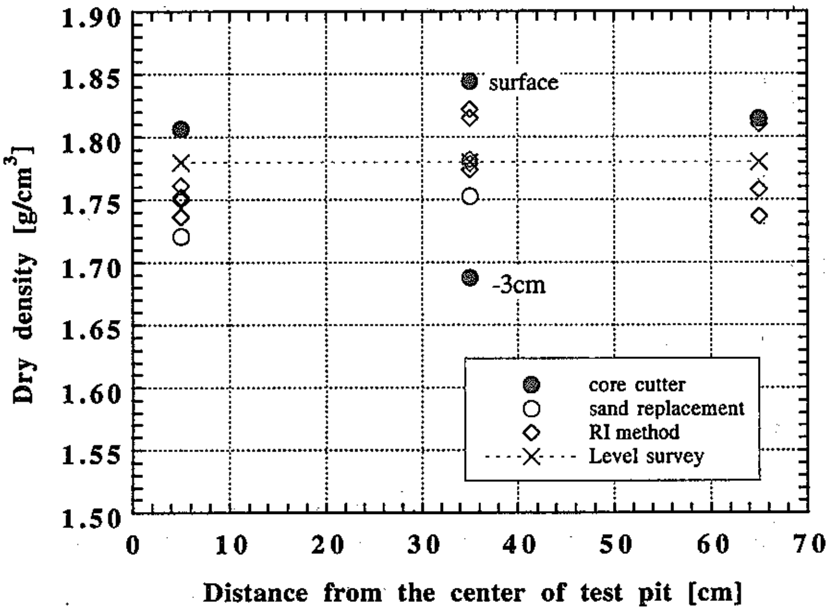

Figure 3-13 Dry density distribution in layer
using some measurement method

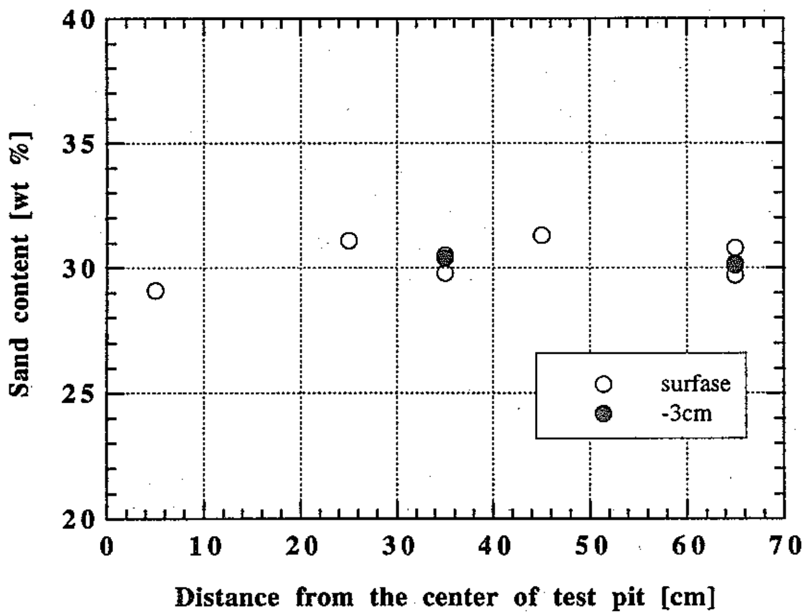

Figure 3-14 Distribution of sand ratio in layer

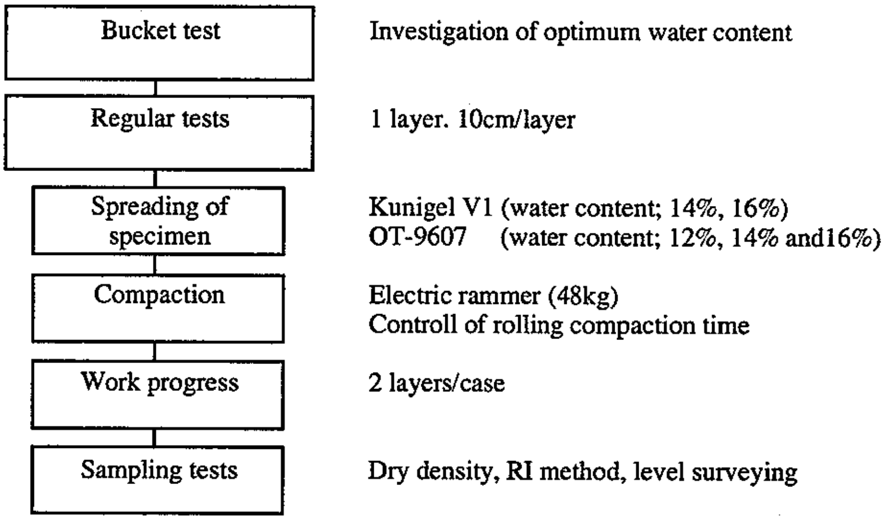

Figure 3-15 Procedure of water content tests

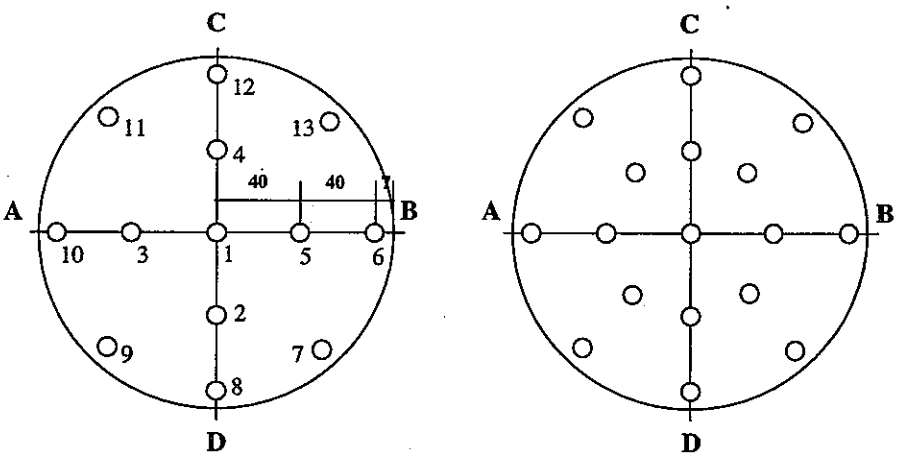

measurement points of RI method

measurement points of level surveying

Figure 3-16 Measurement points on a layer
(water content tests)

Figure 3-17 Schematic view of bucket test

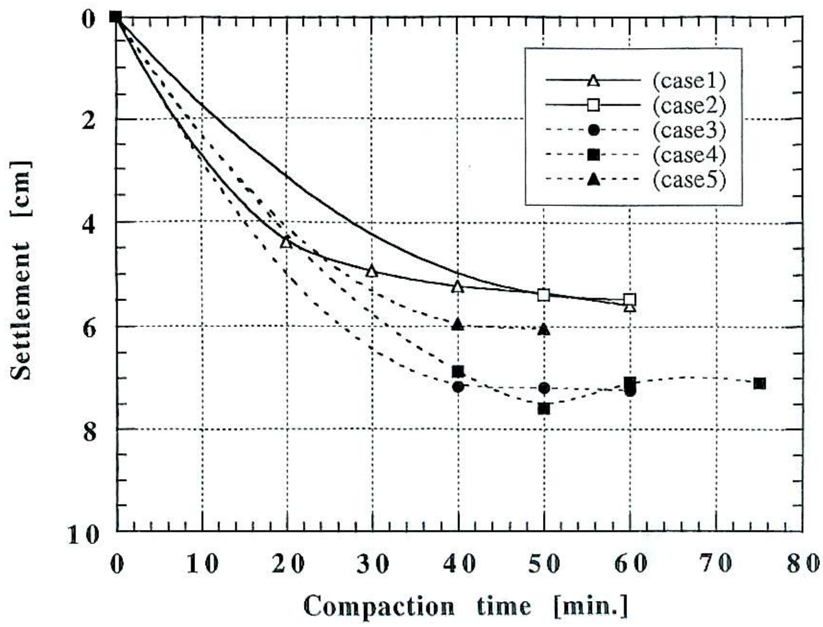

Figure 3-18 Settlement vs compaction time

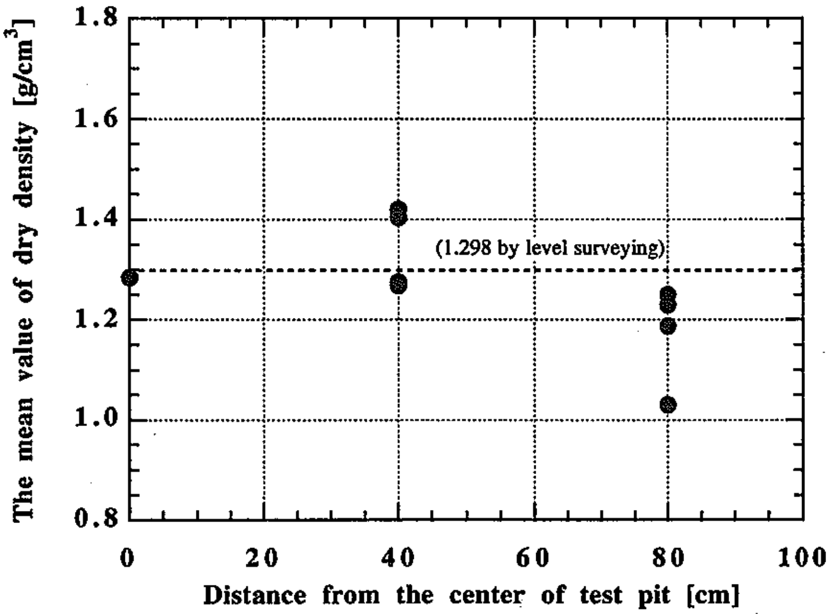

Figure 3-19 Distribution of dry density
(water content test; case1)

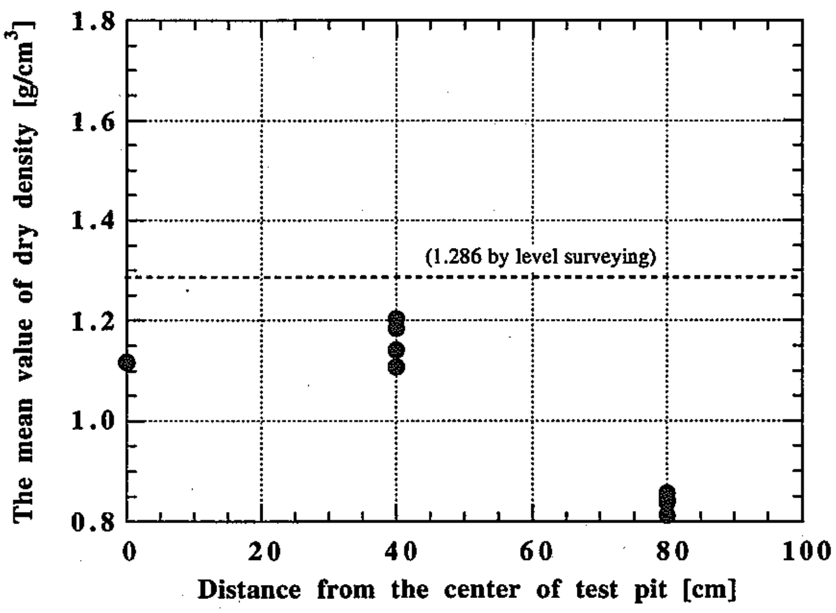

Figure 3-20 Distribution of dry density
(water content test; case2)

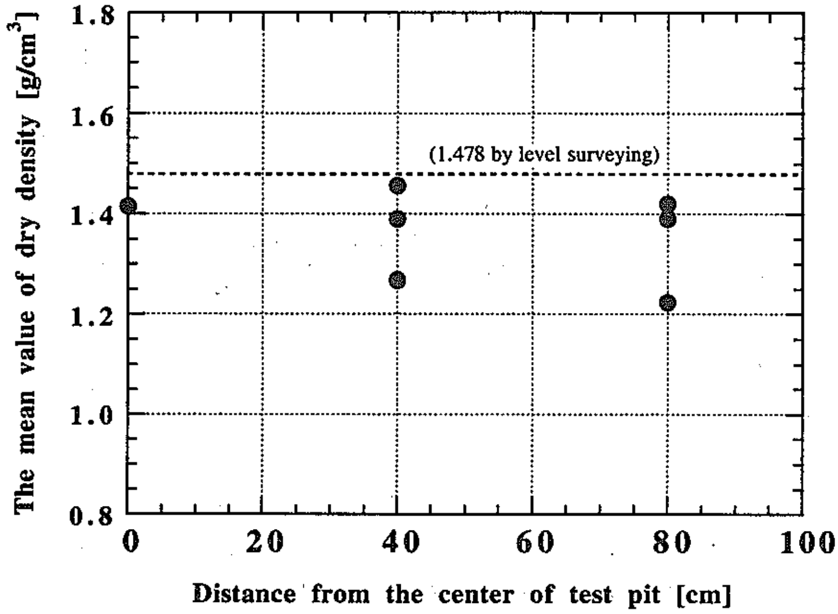

Figure 3-21 Distribution of dry density
(water content test; case3)

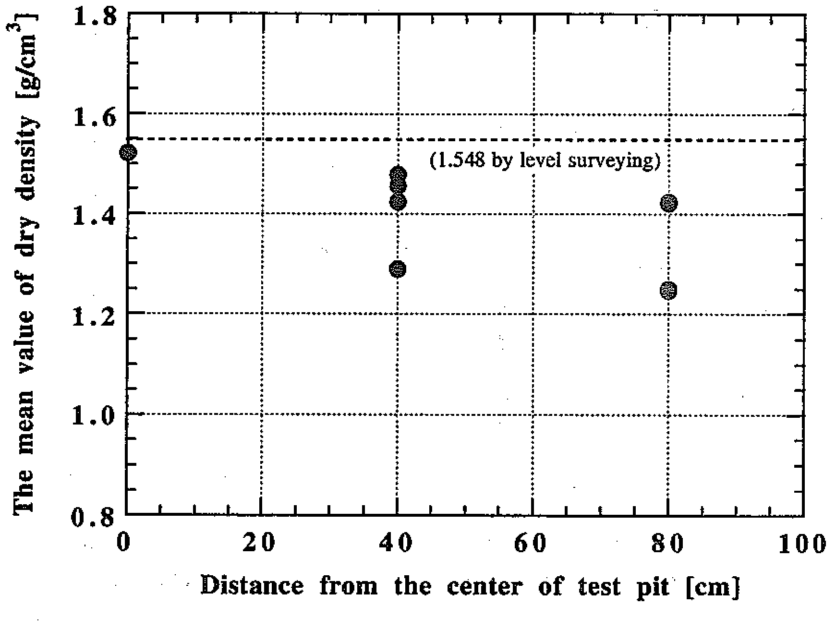

Figure 3-22 Distribution of dry density
(water content test; case4)

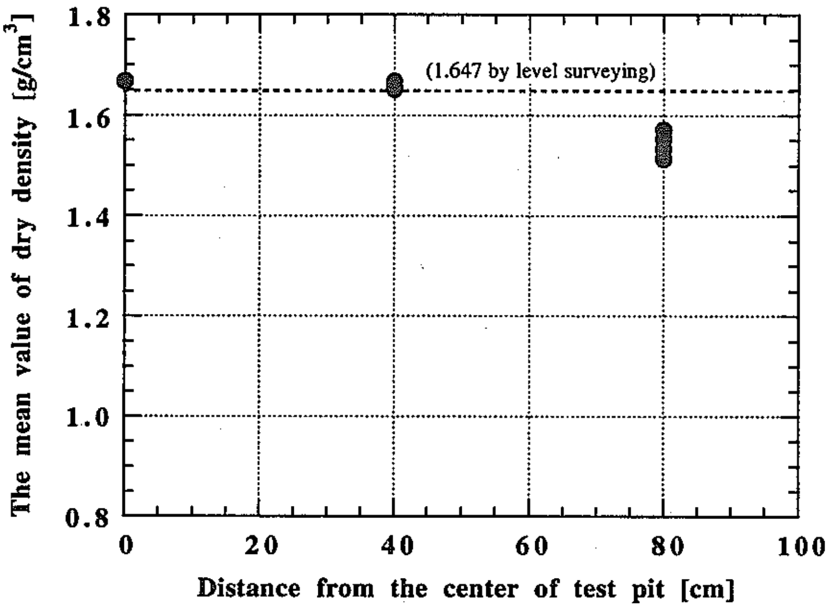

Figure 3-23 Distribution of dry density
(water content test; case5)

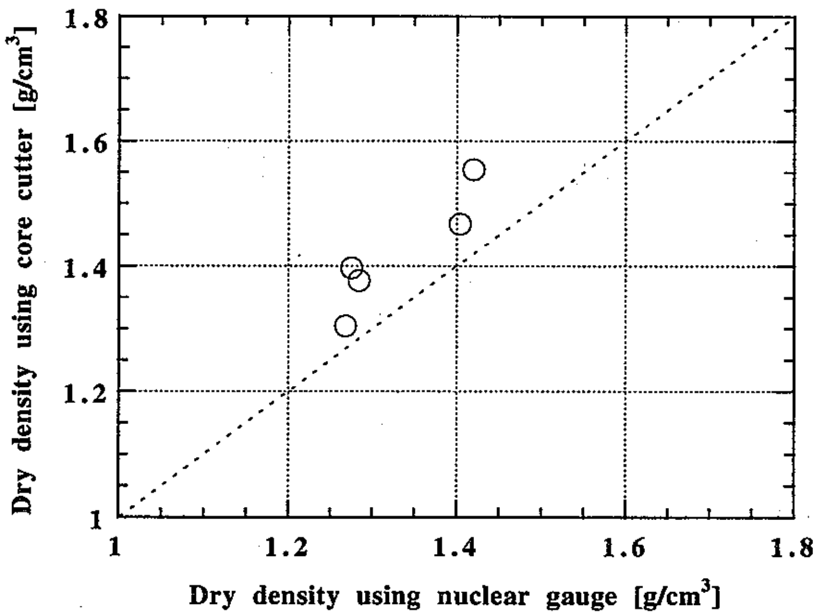

Figure 3-24 Core cutter vs RI method in dry density
(water content test; case1 center of test pit)

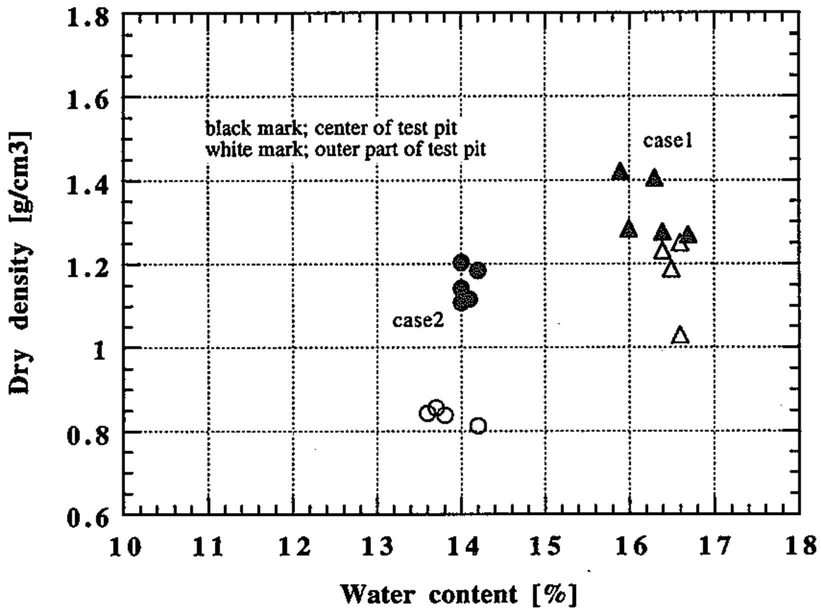

Figure 3-25 Dry density vs water content of Kunigel V1 (water content test)

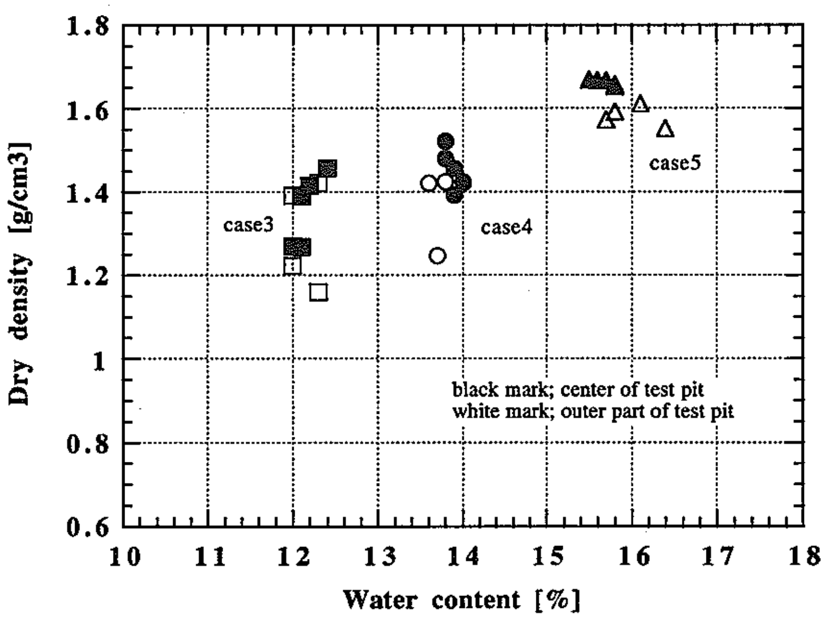

Figure 3-26 Dry density vs water content of OT-9607 (water content test)

4. IN-SITU TEST

4.1 EMPLACEMENT OF THE BUFFER MATERIAL

In-situ test was conducted in the test pit, 1.7 m in diameter and 5.0 m in depth, at Kamaishi experiment (see Figure 2-1). The buffer material for the coupled T-H-M experiment was pure bentonite. The objectives of emplacement technique of the buffer material were as follows:

1) Verification of the in-situ compactible density.
2) Verification of the quality of dry density and water content.

The specimen was OT-9607. Compaction depth of each layer was 10 cm and the initial water content was 15 %.

Compaction machines were the electric rammer and the tamper (Toyo, T-6; see Figure 4-1). The tamper weighs 16.7 kg and the impacting value is 750 per minute. Figure 4-2 shows the situation of compaction of the buffer material. The specimen was spread uniformly and stepped firmly. Two workers operated the rammer.

The controlled dry density determined from the results of the mock-up tests was 1.60 to 1.70 g/cm^3. Figure 4-3 shows the procedure for set up of the buffer material. The compaction of the buffer material started from the bottom of the test pit. Heater annulus was divided into 4 pieces of 1.04 m in diameter and 1.95 m in height. It was installed at the depth of 2.05-4.0 m, and assembled in turn with compaction of the buffer material. The buffer material was set up to the depth of -0.5 m of the test pit. A concrete lid was constructed on the top of the test pit. This lid shut out the direct inflow of water from the pool into the test pit, and the extrusion of the buffer material. On the concrete lid, steel H-piles were installed.

Level surveying was measured to confirm the depth of a layer. Emplacement of the buffer material was one layer a day because of the effort to spread the buffer material, compact it, and measure the level of the surface of the top layer and water content. Treatment between layers involved ripping was shown in Figure 4-5. Therefore, there were many grooves in the interface between layers to evaluate the connection of each layer.

4.2 RESULTS OF EMPLACEMENT OF THE BUFFER MATERIAL

Table 4-1 shows the results of emplacement of the buffer material. The total number of compaction layers was 46. Figure 4-6 shows the relationship between depth of a layer and rolling compaction time.

The compaction area was 1.44 m^2 beside the heater annulus and 2.29 m^2 in the upper and lower sides of heater annulus. Beside the heater annulus, settlement of the buffer material converged quickly. In the upper and lower sides of heater annulus, rolling compaction time scattered in about 60 minutes. This time included the time of the compaction of both the rammer and the tamper.

Figure 4-7 shows the relationship between the depth of a layer and rolling compaction time per unit area. The data scattered randomly. There was no similar relationship between the results of the compaction depth tests and in-situ test. The maximum difference of the compaction time was 40 minutes.

Figure 4-8 shows the relationship between water content of the buffer material and rolling compaction time per unit area. The value of the time was scattered and, there was no clear pattern. It was considered that this scatter of the value included human error, since workers operated the rammer and the tamper.

Figure 4-9 shows the distribution of water content of each layer, and Figure 4-10 shows the histogram of water content of the layers. This water content was the mean value of blended specimen. The mass of the buffer material in one layer was 420 kg. The content of a package was 20 kg. One layer required 21 packages. The water content of one layer was the mean value of these packages. The mean value of the total layers was 14.99 % and standard deviation was 0.911. The scatter of water content was narrow. The water content of 7 layers was beyond the controlled water content.

Figure 4-11 shows the distribution of the compacted dry density of each layer, and Figure 4-12 shows the histogram of the dry density of layers. The mean value of the total layers was 1.653 g/cm^3 and standard deviation was 0.0408. The scatter of the dry density was narrow. The dry density of only 2 layers was out of the controlled dry density. It was considered that the roughness of the bottom of the test pit affected the density of the first and second layers. It was too hard to make the surface of the bottom flat with the rock drill. It was considered that this roughness caused the error of measurement of level surveying. The density of the first layer was high. The average dry density of the first and second layers was the controlled dry density.

This was the reason for a low dry density of the 33rd layer that the work progress after compaction accomplished only to 103 mm.

However, dry density of the 33rd layer was almost 1.6 g/cm^3.

Figure 4-13 shows the relationship between water content and dry density, and there was no clear trend. Dry density scattered in the same water content. These were the same results as the water content tests of the mock-up tests.

Figure 4-14 shows the relationship between level surveying and dry density. Just above the rock mass, the thick layer achieved the highest density. In the other layers, a thin layer achieved the highest density. In the case of the depth of 10 cm of the layer, dry density scattered widely.

Table 4-1 Results of Compaction of the buffer material

No.	Area m^2	Rolling compaction time min.	Time per unit area $min./m^2$	Depth of layer cm	Wet density g/cm^3	Dry density g/cm^3	Water content %
1	2.29	77	33.6	12.35	2.01	1.74	15.6
2	2.29	70	30.6	11.71	1.82	1.57	15.6
3	2.29	70	30.6	9.55	1.95	1.68	15.7
4	2.29	70	30.6	10.40	1.88	1.63	15.6
5	2.29	50	21.8	10.10	1.93	1.67	15.7
6	2.29	45	19.7	10.10	1.84	1.60	15.4
7	2.29	40	17.5	9.70	1.92	1.68	14.7
8	2.29	30	13.1	9.70	1.93	1.68	14.6
9	2.29	40	17.5	10.00	1.88	1.64	14.7
10	2.29	40	17.5	9.50	1.85	1.61	14.4
11	1.44	40	27.8	10.60	1.85	1.61	14.7
12	1.44	30	20.8	9.80	1.92	1.68	14.4
13	1.44	30	20.8	10.10	1.90	1.66	14.3
14	1.44	40	27.8	10.10	1.89	1.65	14.5
15	1.44	30	20.8	10.10	1.90	1.66	14.5
16	1.44	30	20.8	10.10	1.88	1.64	14.8
17	1.44	30	20.8	9.90	1.91	1.66	15.3
18	1.44	20	13.9	9.80	1.91	1.66	15.6
19	1.44	30	20.8	9.90	1.90	1.64	15.6
20	1.44	30	20.8	9.90	1.93	1.67	15.8
21	1.44	50	34.7	10.20	1.87	1.62	15.8
22	1.44	40	27.8	9.70	1.96	1.69	16.1
23	1.44	70	48.6	10.30	1.85	1.60	15.8
24	1.44	30	20.8	9.90	1.90	1.64	15.9
25	1.44	30	20.8	10.00	1.87	1.62	15.8
26	1.44	30	20.8	10.00	1.89	1.63	16.0
27	1.44	40	27.8	9.90	1.91	1.66	15.1
28	1.44	20	13.9	7.60	1.95	1.71	14.2
29	1.44	20	13.9	8.00	1.89	1.65	14.1
30	1.44	20	13.9	7.70	1.97	1.73	13.9
31	2.29	50	21.8	6.20	1.97	1.73	14.1
32	2.29	45	19.7	10.10	1.85	1.62	14.2
33	2.29	85	37.1	10.30	1.81	1.58	14.6
34	2.29	90	39.3	9.70	1.92	1.67	15.0
35	2.29	55	24.0	10.00	1.87	1.61	15.7
36	2.29	45	19.7	9.90	1.87	1.62	15.8
37	2.29	50	21.8	10.10	1.88	1.62	15.9
38	2.29	75	32.8	10.10	1.94	1.68	15.1
39	2.29	80	34.9	10.20	1.91	1.67	14.7
40	2.29	30	13.1	9.80	1.82	1.60	13.8
41	2.29	50	21.8	9.60	1.83	1.61	13.7
42	2.29	60	26.2	9.90	1.97	1.72	14.1
43	2.29	60	26.2	10.00	1.96	1.69	15.8
44	2.29	60	26.2	10.00	1.97	1.69	16.4
45	2.29	60	26.2	10.00	1.97	1.71	15.1
46	2.29	80	34.9	10.70	1.85	1.66	11.3
Total				453.31			
Mean					1.901	1.653	14.99
Standard deviation					0.0476	0.0408	0.9110

Figure 4-1 The Tamper

Figure 4-2 Compaction of the buffer material

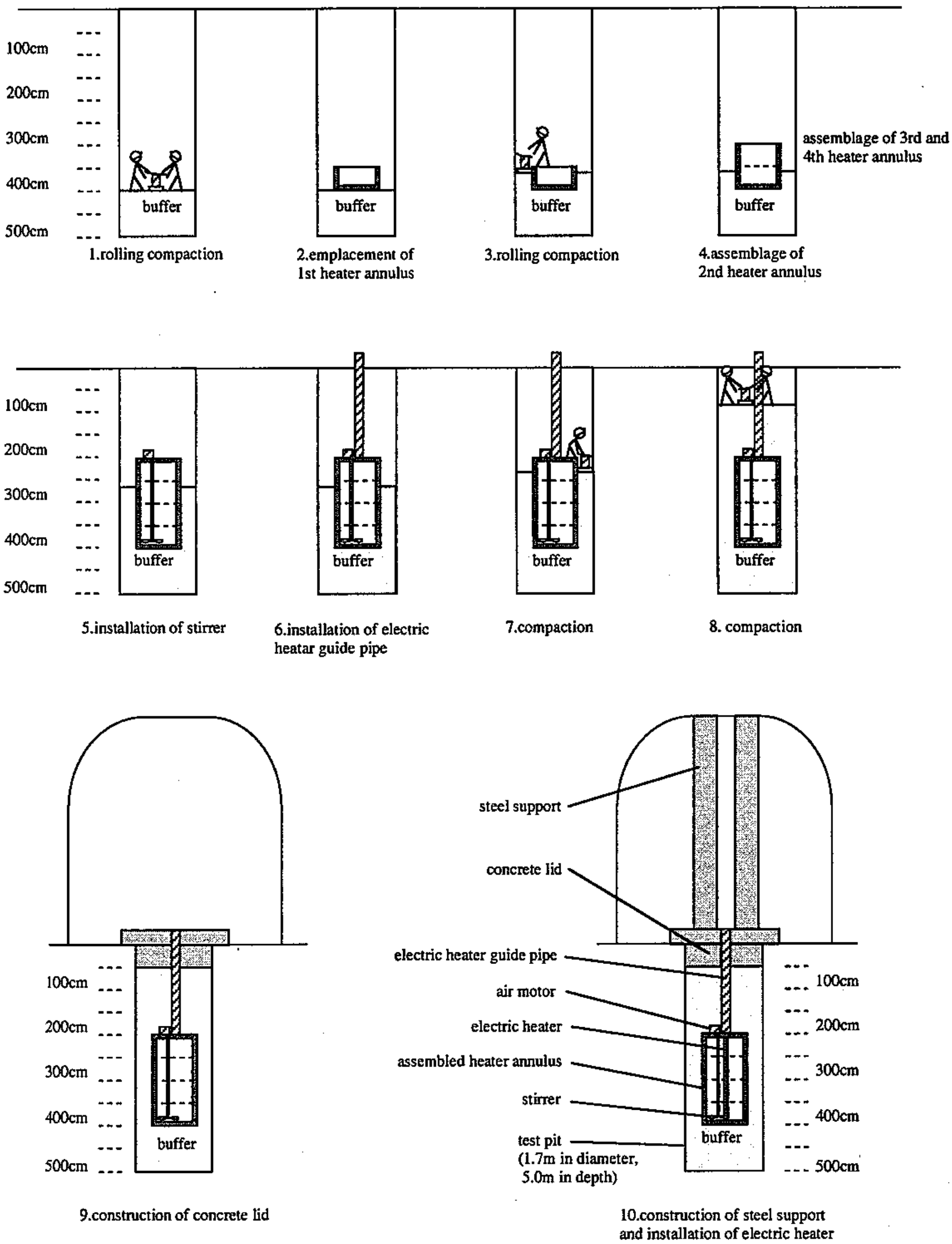

Figure 4-3 Procedure of set up of the buffer material

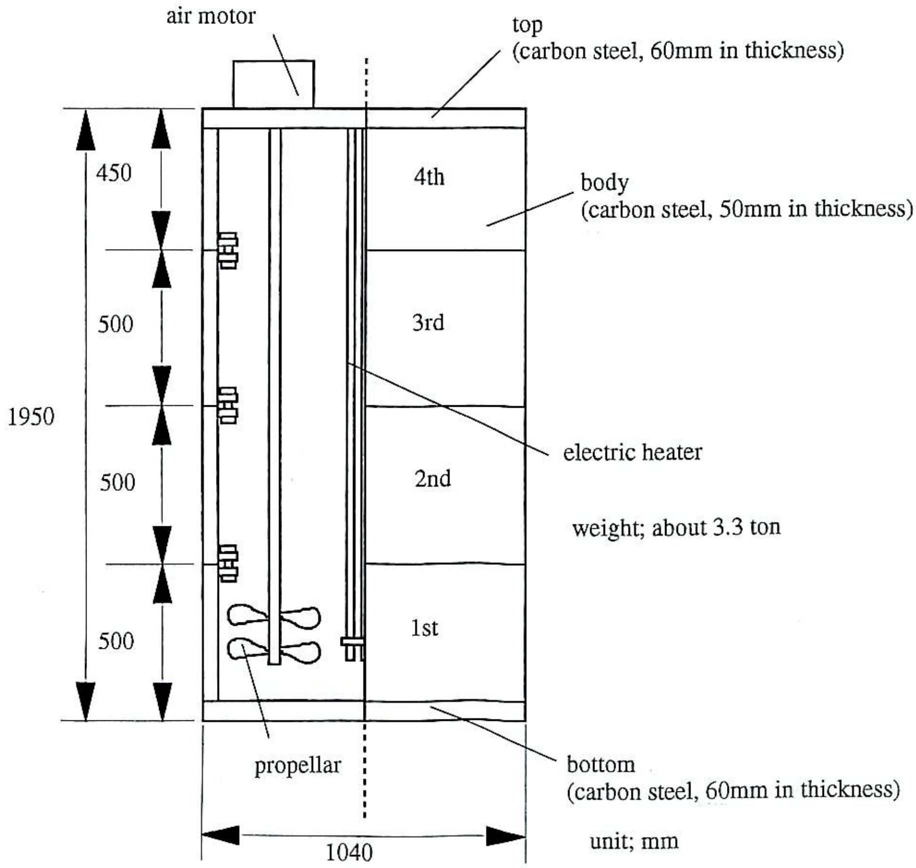

Figure 4-4 Heater annulus

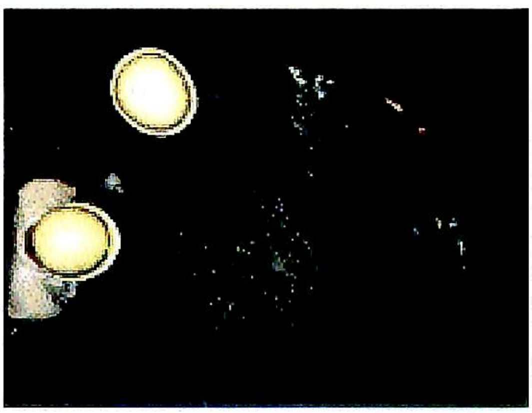

Figure 4-5 Ripping of the surface of the compacted buffer

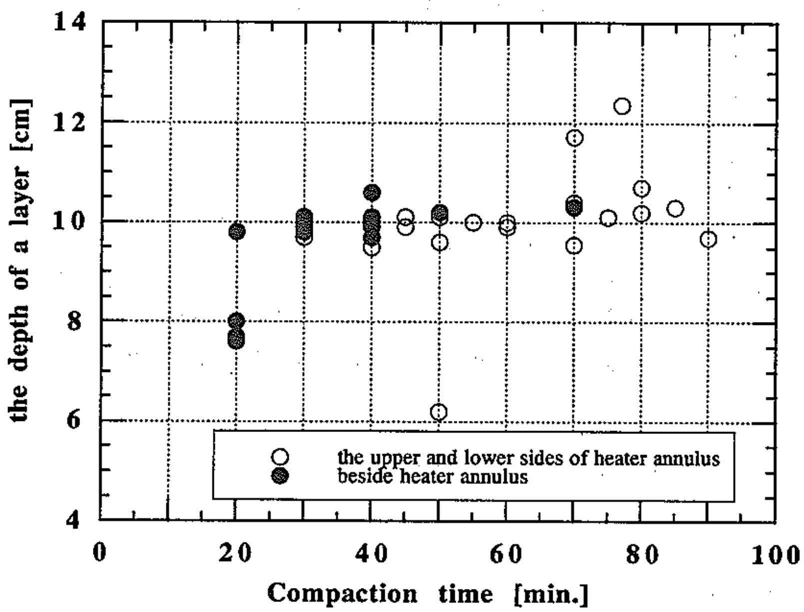

Figure 4-6 The depth of a layer vs compaction time

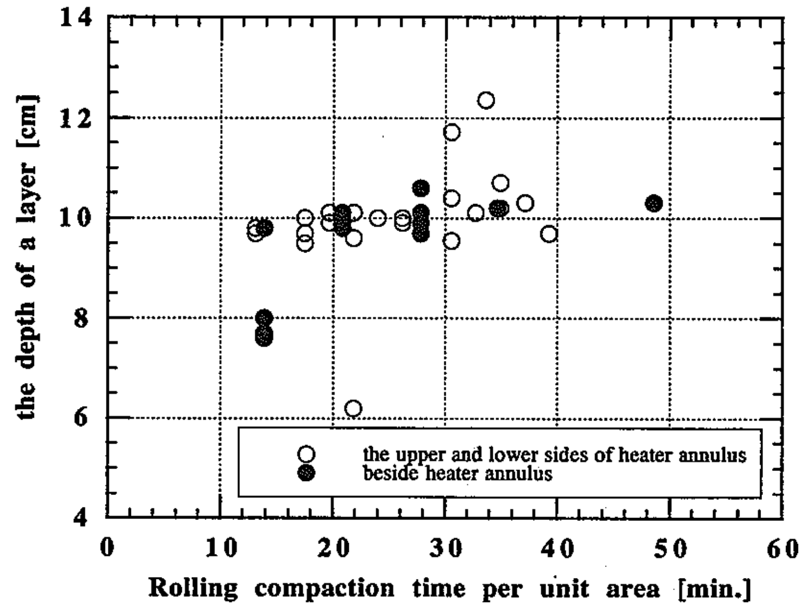

Figure 4-7 The depth of a layer vs rolling compaction time per unit area

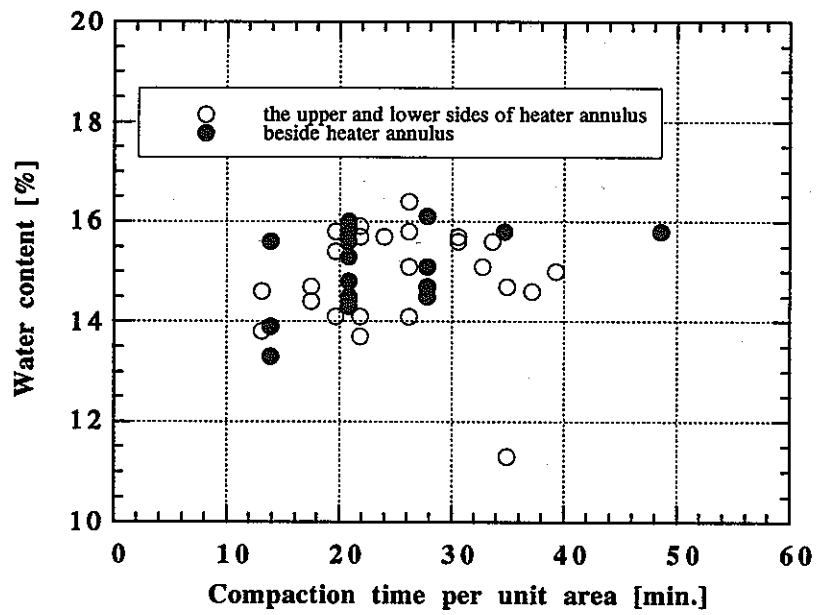

Figure 4-8 Water content vs compaction time per unit area

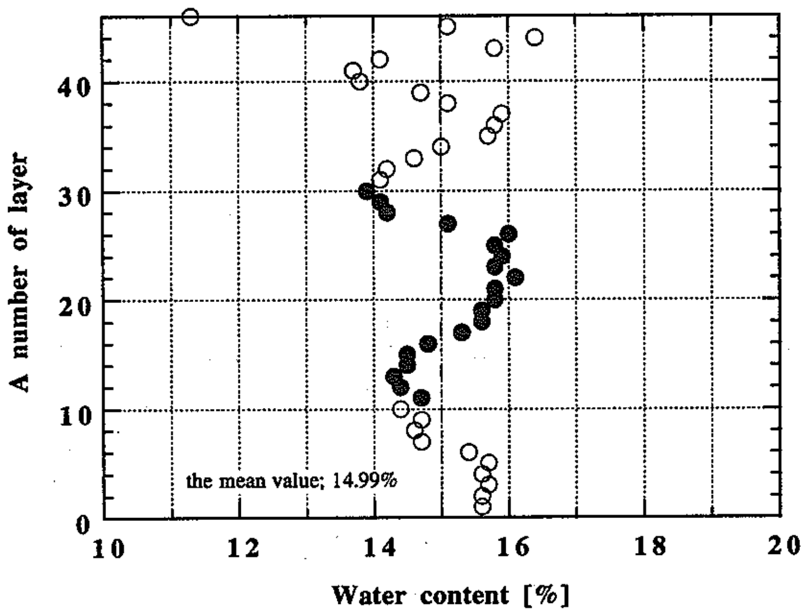

Figure 4-9 Water content of each layer

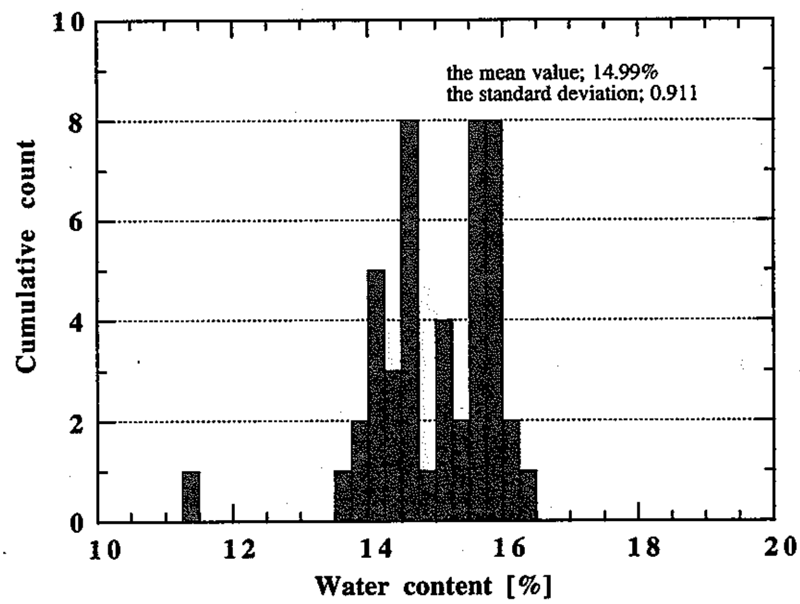

Figure 4-10 Histogram of water content of each layer

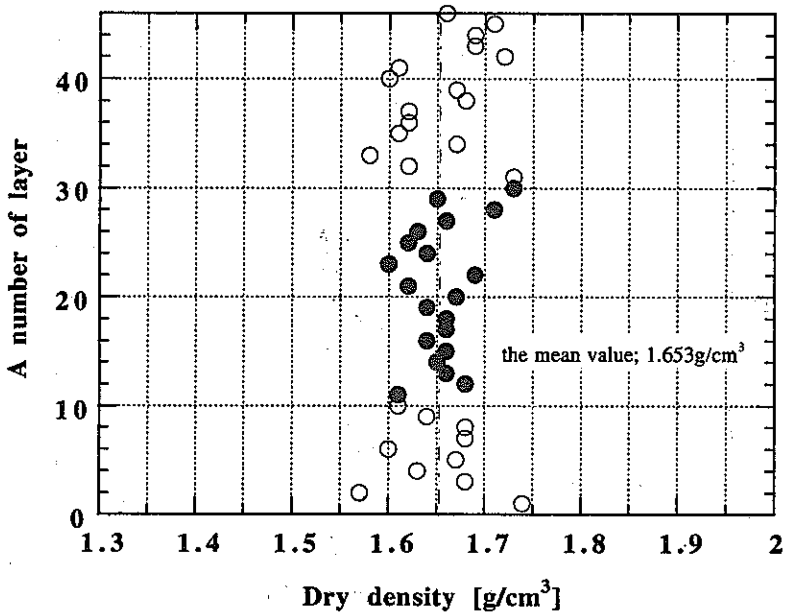

Figure 4-11 Dry density of each layer

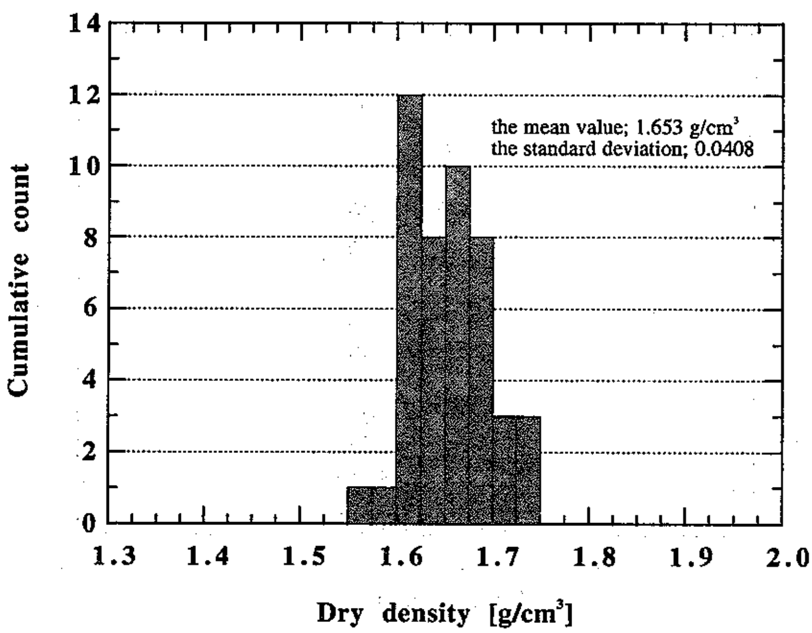

Figure 4-12 Histogram of dry density of each layer

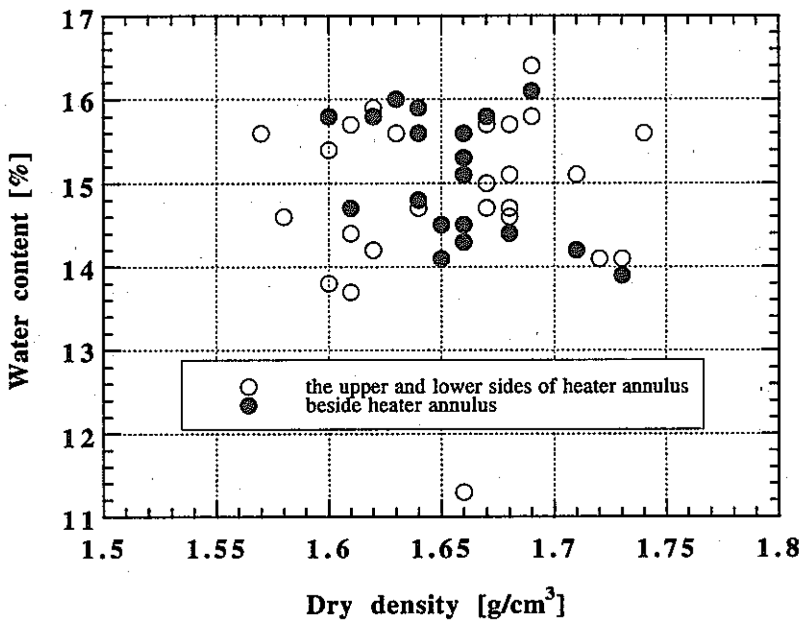

Figure 4-13 Water content vs dry density

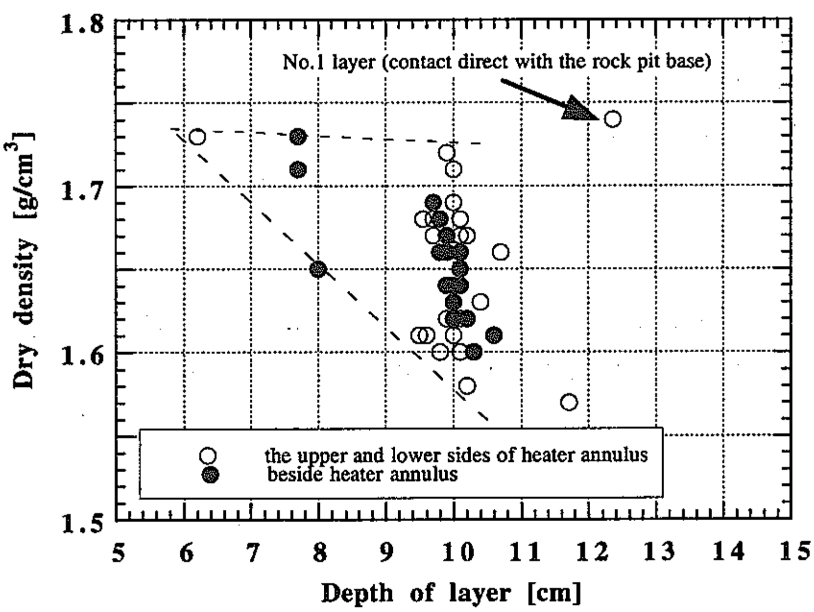

Figure 4-14 Dry density vs depth of layer

5. CONCLUSION

The in-situ direct compaction technique which was one of the major candidate emplacement techniques of the buffer material was conducted to evaluate the appropriate conditions and the quality of the compacted layers. This experiment consisted of the mock-up tests and the in-situ test. The mock-up tests showed the appropriate conditions for the in-situ direct compaction technique as follows:

1) Appropriate compaction depth for each layer with compaction of the buffer material by the electric rammer was 10 cm.
2) The necessary time for compaction of the buffer material of each layer in the test pit, which was 1.7 m in diameter, was about 60 minutes.
3) Uniform spreading of bentonite sample produced a uniform layer.
4) Bentonite sample with the optimum water content was effective in achieving a high dry density.
5) In bentonite clay, OT-9607 achieved high dry density of 1.65 g/cm^3.
6) In bentonite-sand mixture, the sands were scattered uniformly in the layer.

In-situ experiment, the manufactured OT-9607 achieved dry density with a mean value was 1.65 g/cm^3 which the coupled thermo-hydro-mechanical experiment demanded.

ACKNOWLEDGEMENT

Authors would like to thank Dr. Amemiya, HAZAMA Corporation, and Mr. Takiguchi, TOHO Drilling Equipment, for their works.

REFERENCES

Fujita, T., Sugita, Y., Sato, T., Ishikawa, H. and Mano, T. (1994) : Coupled thermo-hydro-mechnical experiment at Kamaishi Mine, Technical Note 01-95-01, plan, PNC TN8020 94-005.

Fujita, T., Chijimatsu, M., Ishikawa, H., Suzuki H. and Matsumoto, K. (1997) : Coupled thermo-hydro-mechnical experment at Kamaishi Mine, Technical Note 11-96-04, Fundamental Properties of Bentonite OT-9607, PNC TN8410 97-071.

Gunnarsson, D., Johannesson, L., Sandén, T. and Börgesson, L. (1996) : Field test of tunnel backfilling, Progress report, HRL-96-28.

Japanese Geotechnical Society (1995) : Guideline of subsurface investigation. (in Japanese)

Kjartanson, B.H., Chandler, N.A., Wan, A.W.L., Radhakrishna, H.S. and Lau, K.-C. (1993) : In Situ Assessment of Bentonite/Sand Buffer Material, Joint CSCE-ASCE National Conference on Environmental Engineering, pp. 747-755.

Neerdael, B., Meynendonckx, P. and Voet, M. (1992) : The Bacchus backfill experiment at the Hades underground research facility at Mol, Belgium, Final Report, EUR 14155.

Pusch, R. and Börgesson, L., (1985) : Final report of the buffer mass test - volume II, SKB Technical report 85-12.

Sato, S., Kobayashi, A., Hara, K., Ishikawa, H. and Sasaki, N. (1991) : Full Scale Test on Coupled Thermo-Hydro-Mechnical Process in Engineered Barrier System, Proc. of '91 Joint Int. Waste Management Conference, ASCE, Seoul.

Sugita, Y., Fujita, T. and Kanno, T. (1995) : Adherence test of buffer material using spraying method, PNC TN8410 95-179.(in Japanese)